

ABSTRACT

MALOTKY, ERICA LOUISE. Functional Characterization of MoeA and MoeB Tungsten Cofactor Synthesis Proteins from the Hyperthermophilic Archaeon *Pyrococcus furiosus*. (Under the direction of Amy Grunden)

The hyperthermophilic archaeon, *Pyrococcus furiosus* depends on the element tungsten for growth since tungsten-containing enzymes such as aldehyde ferredoxin oxidoreductase (AOR) are key to its metabolism. Crystal structure analysis of the tungsten cofactor in AOR indicated that the tungsten cofactor exists as part of a tricyclic pterin moiety analogous to molybdopterin cofactor present in molybdoenzymes such as nitrate reductase. Molybdopterin cofactor synthesis has been well characterized in *Escherichia coli* with the identification of at least 14 genes that participate in this process. Analysis of the *P. furiosus* genome revealed that it has homologs to all cofactor synthesis genes except for *modE*, a transcriptional regulator of molybdopterin cofactor synthesis, and *mogA*, a putative molybdo-chelator. Two of the molybdenum cofactor biosynthesis genes, *moeA* and *moeB*, involved in activation of molybdenum and in donation of sulfur to the pterin ring structure, respectively, each have two homologs in *P. furiosus* (MoeA, 45%, MoeA2, 44%, MoeB, 50%, and MoeB2, 47% similar to *E. coli* MoeA and MoeB respectively). The MoeA and MoeB homologs were targeted for initial functional activity studies to determine if they participate in cofactor formation. The activity studies entailed complementing *E. coli* strains mutant in *moeA* or *moeB* with recombinant *P. furiosus* homologs in an in vitro

system and assaying for restoration of the molydoenzyme nitrate reductase (NR) activity. Partial complementation of defects in *E. coli moeA* and *moeB* were observed for assays including *P. furiosus* MoeA2 and MoeB2 which supported 13.1 nmole $\text{NO}_2^- \cdot \text{min}^{-1} \cdot \text{mg}^{-1}$ (10 μg MoeA2) and 19.6 nmole $\text{NO}_2^- \cdot \text{min}^{-1} \cdot \text{mg}^{-1}$ (100 μg MoeB2) activity respectively. These specific activities represent 10.1% and 15.1% of wild type *E. coli* nitrate reductase activity (130 nmole $\text{NO}_2^- \cdot \text{min}^{-1} \cdot \text{mg}^{-1}$) Only negligible restoration of nitrate reductase activity was observed when *P. furiosus* MoeA or MoeB was included in the assay, with specific activities 0.16 nmole $\text{NO}_2^- \cdot \text{min}^{-1} \cdot \text{mg}^{-1}$ (1 μg MoeA) and 0.74 $\text{NO}_2^- \cdot \text{min}^{-1} \cdot \text{mg}^{-1}$ (50 μg MoeB). Partial complementation of the *E. coli moeA* mutant was also observed for *in vitro* trimethyl amine oxide (TMAO) reductase assays where 10 μg MoeA2 supported a specific activity of 40.97 nmole TMAO reduced $\cdot \text{min}^{-1} \cdot \text{mg}^{-1}$ and 10 μg MoeB2 supported a specific activity of 6.3 nmole TMAO reduced $\cdot \text{min}^{-1} \cdot \text{mg}^{-1}$ compared to 2,374 nmole TMAO reduced $\cdot \text{min}^{-1} \cdot \text{mg}^{-1}$ for the wild type *E. coli*. When TMAO assays were conducted in the presence of tungsten rather than molybdenum, the wild type *E. coli* had a specific activity of 1,297 nmole TMAO reduced $\cdot \text{min}^{-1} \cdot \text{mg}^{-1}$. *E. coli moeA* mutant had an activity of 2.07 nmole TMAO reduced $\cdot \text{min}^{-1} \cdot \text{mg}^{-1}$ when supplemented with 10 μg MoeA2 and the *E. coli moeB* mutant supported 6.01 nmole TMAO reduced $\cdot \text{min}^{-1} \cdot \text{mg}^{-1}$ when supplemented with 100 μg MoeB2. The partial nature of the complementation seen in these studies is likely due in part to the use of sub optimal assay temperatures (37°C), as required for *E. coli* NR, well below the optimum temperature of 95°C seen for most *P. furiosus* enzymes. Nevertheless,

these complementation assays demonstrate that *P. furiosus* MoeA2, and MoeB2 homologs likely function as MoeA and MoeB in tungsten cofactor synthesis in *P. furiosus*.

**Functional Characterization of MoeA and MoeB Tungsten
Cofactor Synthesis Proteins from the Hyperthermophilic
Archaeon *Pyrococcus furiosus***

by

Erica Louise Malotky

A thesis submitted to the Graduate Faculty of North Carolina State University
in partial fulfillment for the Degree of Master of Science

Microbiology

Raleigh

2002

Approved By:

Stephen Libby

James Brown

Chair of Advisory Committee
Amy Grunden

Biography

Erica Louise Malotky was born to Susanne and Lyle Malotky in Washington, DC on August 11th 1978. She grew up in Fort Washington Maryland where she attended Fort Washington Forrest Elementary School and Eugene Burroughs Middle School. In 1992 Erica was admitted to the science and technology program at Oxon Hill High School where, in addition to soccer and swimming, biology sparked an interest. Her interest for swimming and biology continued through college. Erica entered Salisbury University in 1996; she was a member of the swim team, she majored in biology and received a minor in chemistry. Erica graduated from Salisbury University in 2000. In July 2000 she left Maryland and moved to Raleigh, NC to work towards her MS in Microbiology.

Acknowledgments

Many thanks to Dr. Stephen Libby and Dr. James Brown for serving on my advisory committee. Thanks to the Libby lab and the Hassan lab for letting me use their equipment and materials. Thank you to Mikyoung Ji, Karen Kast-Hutcheson, Erika Johnson and Elizabeth Boutt for keeping me sane at work. Thank you to Jill Garroway, Carrie Lee, Lisa Cook and especially Bryan Scappini for believing in me and listening to my lab stories. A special thanks to Dr. Amy Grunden, first for letting me in her lab, for teaching me metabolic pathways can be fun and for being by my side the whole step of the way. Last I would like to thank my family, especially my mom and dad, for their endless support.

Table of Contents

List of Tables.....	v
List of Figures.....	vi
Background.....	1
Materials and methods.....	13
Results.....	22
Discussion.....	53
Literature cited.....	65

List of Tables

Table 1. <i>P. furiosus</i> homologs.....	12
Table 2. Bacterial strains used in this study.....	21
Table 3. In Vivo complementation of <i>E.coli moeA</i> mutations with <i>P. furiosus</i> MoeA, MoeA2 determined by restoration of nitrate reductase activities.....	42
Table 4. <i>In vitro</i> TMAO reductase assay for <i>P. furiosus</i> MoeA2 with molybdenum.	43
Table 5. <i>In vitro</i> TMAO reductase assay for <i>P. furiosus</i> MoeA2 with tungsten.....	44
Table 6. <i>In vitro</i> TMAO reductase assay for <i>P. furiosus</i> MoeB2 with molybdenum.....	45
Table 7. <i>In vitro</i> TMAO reductase assay for <i>P. furiosus</i> MoeB2 with tungsten.....	46
Table 8. Average threshold cycle for individual tungsten cofactor synthesis genes with various amounts of tungsten.....	50
Table 9: Average mRNA copy number for individual tungsten cofactor synthesis genes with various amounts of tungsten.....	51

List of Figures

Figure 1. Mo cofactor synthesis.....	11
Figure 2. Recombinant <i>P. furiosus</i> Protein purification using the metal chelation column.....	32
Figure 3. <i>P. furiosus</i> MoeA2 purification protein gel.....	33
Figure 4. <i>P. furiosus</i> MoeB2 purification protein gel.....	34
Figure 5. All of the purified <i>P. furiosus</i> proteins.....	35
Figure 6. <i>In vitro</i> nitrate reductase assay with <i>P. furiosus</i> MoeA, <i>P. furiosus</i> MoeA2 and <i>E.coli</i> MoeA.....	36
Figure 7. <i>In vitro</i> TMAO reductase assay with <i>P. furiosus</i> MoeA2 and molybdenum.....	37
Figure 8. <i>In vitro</i> TMAO reductase assay with <i>P. furiosus</i> MoeA2 and tungsten.....	38
Figure 9. <i>In vitro</i> nitrate reductase with <i>P. furiosus</i> MoeB, MoeB2, <i>E. coli</i> MoeB and ThiF.....	39
Figure 10. <i>In vitro</i> TMAO reductase assay with <i>P. furiosus</i> MoeB2 and molybdenum.....	40
Figure 11. <i>In vitro</i> TMAO reductase assay with <i>P. furiosus</i> MoeB2 and tungsten.....	41
Figure 12. Standard curve for the real time RT-PCR experiments.....	47

List of figures (cont)

Figure 13. Real time RT-PCR threshold cycle data for cells grown in 1 nM tungsten.....	48
Figure 14. Real time RT-PCR melting curve for cells grown in 1 nM tungsten.....	49
Figure 15. Tungsten cofactor synthesis gene expression levels in response to varying amounts of tungsten in the growth media.....	50
Figure 16. Alignment of <i>P. furiosus</i> MoeA with <i>E. coli</i> MoeA.....	59
Figure 17. Alignment of <i>P. furiosus</i> MoeA2 with <i>E. coli</i> MoeA.....	60
Figure 18. Alignment of <i>P. furiosus</i> MoeB with <i>E. coli</i> ThiF.....	61
Figure 19. Alignment of <i>P. furiosus</i> MoeB with <i>E. coli</i> MoeB.....	62
Figure 20. Alignment of <i>P. furiosus</i> MoeB2 with <i>E. coli</i> ThiF.....	63
Figure 21. Alignment of <i>P. furiosus</i> MoeB with <i>E. coli</i> MoeB.....	64

Background

Until the late 1970's it was thought that life could not exist at temperatures above 70°C. However, in the early 1980s Stetter and coworkers discovered hyperthermophiles, organisms with optimum growth temperatures of at least 80°C and a maximum growth temperature of 90°C or above (Stetter, 1996). These organisms are mainly isolated from marine geothermal environments, which include both shallow and deep hydrothermal vents (Adams 1999). One of these hyperthermophiles, *Pyrococcus furiosus*, is a strict anaerobic heterotroph that grows either saccharolytically on starch, glycogen or maltose or proteolytically on peptides and has an optimal growth temperature of 100°C (Fiala and Stetter, 1986). By analysis of 16S ribosomal RNA, it was determined that this organism can be classified as an Archaea (formerly Archaeobacteria), a grouping of organisms which constitute the third domain of life (Woese *et al.* 1990). Archaea contain genes that encode both bacterial- and eucaryotic-like proteins, thus indicating Archaea are related to, but are distinct from, the other two domains (Woese *et al.* 1990). The hyperthermophilic Archaea are one of the most slowly evolving organisms within their domain. This suggests that the original organisms on this planet may have evolved under high temperature, and if this is true, studying hyperthermophiles could offer a vast amount of information about the evolution of enzymes and metabolic pathways (Stetter 1996).

From initial biochemical and physiological studies of *P. furiosus*, it has been determined that the element tungsten, an analog of molybdenum, is required for growth (Mukund and Adams, 1996). Tungsten is present in low concentrations in normal seawater, however there is a greater abundance of tungsten near the deep sea hydrothermal vents.

Tungsten is known to be present in samples of vent fluids at about one thousand times that found in normal seawater (Arnulf and Adams 1996).

This obligate tungsten requirement is most likely in part due to the replacement in *P. furiosus* of the classical glycolytic enzyme glyceraldehyde-3-phosphate dehydrogenase with the tungsten-containing enzyme glyceraldehyde-3-phosphate:ferredoxin oxidoreductase (Mukund and Adams, 1995). Furthermore, the involvement of the tungsten containing enzymes formaldehyde:ferredoxin oxidoreductase (FOR) (Roy *et al.* 1999) and aldehyde:ferredoxin oxidoreductase (AOR) (Mukund and Adams, 1991) in peptidolytic metabolism, where FOR functions in the catabolism of basic amino acids and AOR in the oxidation of reactive aldehydes generated during 2-keto acid conversion, respectively, would explain a tungsten growth requirement when *P. furiosus* is cultured using peptides as the carbon source. Interestingly, it has been shown that while *P. furiosus* exhibits tungsten-growth dependence, molybdenum is not required and cannot be used *in vitro* to substitute for tungsten in active *P. furiosus* tungstoenzymes (Mukund and Adams, 1996). This dependence on tungsten rather than molybdenum has been observed for other thermophiles and hyperthermophiles (Adams, 1999), suggesting that the tungsten form of the enzymes may be more thermally stable (Kletzin and Adams, 1996). The increased thermostability of a tungsten- versus molybdenum-containing enzyme has in fact been observed in the case of the *E. coli* molybdoenzyme trimethylamine oxide (TMAO) reductase (Buc *et al.* 1999). Studies by Buc *et al* have shown that maximal activity of the molybdenum TMAO reductase was reached at 60°C while the maximal level for tungsten TMAO reductase activity was attained at 80°C (Buc *et al.* 1999).

Structural studies of *P. furiosus* tungstoenzymes have demonstrated that their tungsten centers exist as a part of a bis-pterin cofactor, which is similar to the bis-pterin molybdenum cofactor (MPT) seen in mesophilic molybdoenzymes such as nitrate reductase and TMAO reductase (Kletzin and Adams, 1996; Chan *et al.*, 1995; Rajagopalan and Johnson, 1992). The biosynthesis of the molybdenum cofactor has been almost completely characterized in the mesophilic bacteria *Escherichia coli* and *Rhodobacter capsulatus* (Figure 1). However it should be noted that many mesophilic molybdoenzymes have a guanine dinucleotide moiety attached to the MPT that has not been observed to be present in any of the tungsten enzymes structurally characterized to date.

The process of MPT synthesis is generally considered to occur in three phases. The early steps entail the conversion of a guanosine derivative, most likely GTP, to Precursor Z through the action of enzymes MoaA, MoaB, and MoaC (Wuebbens and Rajagopalan, 1995; Rieder *et al.*, 1998). The next steps involve the conversion of Precursor Z into molybdopterin (MPT), thereby producing the dithiolene group required for molybdenum coordination. This transformation is catalyzed by the two-subunit enzyme molybdopterin synthase encoded by the *moaDE* genes (Pitterle and Rajagopalan, 1993). During Precursor Z conversion to MPT, the C-terminus of the MoaD subunit of MPT synthase is altered to a glycine thiocarboxylate, which appears to function as the S donor for the dithiolene group addition to MPT (Pitterle *et al.*, 1993). MPT synthase then regains its sulfur ligand through sulfurylation by MoeB (Rajagopalan, 1997). The final steps of cofactor synthesis involve the attachment of molybdenum, which has been transported into the cell in the form of the Mo oxyanion (MoO_4^{2-}) via the molybdate-specific ModABC transporter. Upon entering the cell, molybdate is activated by MoeA and attached to MPT (Hasona *et al.*, 1998) probably through

docking with the proposed molybdochelator MogA (Joshi *et al.*, 1996). MPT can be further processed by the attachment of a guanosine dinucleotide moiety to MPT by MobA to form the molybdopterin guanine dinucleotide form of the cofactor (MGD) (Johnson *et al.*, 1991; Palmer *et al.*, 1996). All of the molybdoenzymes in *E. coli* require the MGD form of the cofactor, whereas all of the *P. furiosus* tungstoenzymes characterized to date appear to contain a bispterin MPT form of the cofactor (Kletzin and Adams, 1996; Roy *et al.*, 1999).

In *E. coli* and other mesophilic bacteria the process of molybdenum cofactor biosynthesis is shown to be transcriptually regulated by the molybdate-bound form of the ModE protein (ModE-Mo) (Grunden *et al.*, 1996, McNicholas *et al.* 1997, Grunden *et al.* 1999, Anderson *et al.* 2000). Specifically ModE-Mo regulates the expression of the molybdate transporter (Grunden *et al.* 1999) as well as the synthesis of *moa* genes (Anderson *et al.* 2000). In addition to its role as a repressor of molybdate transport genes, ModE-Mo also enhances the expression of genes coding for molybdoenzymes such as nitrate reductase, formate dehydrogenase and dimethylsulfoxide reductase (Self *et al.* 1999)

Given that tungsten functions as a chemical analog of molybdenum and that the tungsten centers in *P. furiosus* tungstoenzymes are remarkably similar to MPT cofactor found in molybdoenzymes, it is reasonable to predict that tungsten cofactor biosynthesis proceeds in *P. furiosus* in a fashion similar to that seen for MPT biosynthesis. An analysis of the *P. furiosus* genome identified a number of MPT biosynthesis homologs, which exhibit from 41 to 63% similarity to known MPT biosynthesis genes (Table 1). It should be noted that *P. furiosus* seem to possess homologs for every required step of the MPT biosynthetic process but does not appear to have any obvious homologs of the molybdate-specific

periplasmic binding protein (*modA*) or the putative molybdenum chelator *mogA*. *P. furiosus* also does not seem to have a homolog to the molybdenum cofactor synthesis regulator *modE*.

In order to begin to ascertain whether tungsten cofactor biosynthesis occurs in a fashion similar to molybdocofactor synthesis, the true function of the putative tungsten cofactor synthesis genes must be explored. For these studies, *P. furiosus* MoeA and MoeB were initially targeted for investigation for a number of reasons. As it can be seen in Table 1, there are two proposed homologs for both MoeA and MoeB. In order to understand the cofactor biosynthesis, it has to be determined which, if any of the proposed *P. furiosus* homologs function as the true homolog. Also, MoeA is of great interest due to its involvement in activating the metal for insertion into the cofactor. This would likely be a step in cofactor synthesis that may be metal specific and could therefore be a point in the synthesis process that would clearly differentiate molybdenum from tungsten cofactor synthesis. Lastly, there are *E. coli* strains available that have mapped mutations in *moeA* and *moeB* that can be used for assessment of function of the *P. furiosus* homologs through complementation studies.

moeA and *moeB* genes are both located in the *E. coli* *moe* operon. (Nohno *et al.* 1998). In *E. coli*, MoeA is involved in the final step of the molybdenum cofactor (MoCo) biosynthesis: the incorporation of molybdenum into molybdopterin (Hasona *et al.* 1998). *E. coli* MoeB is involved in the synthesis of the molybdopterin, this is accomplished by sulfurylating the small subunit of the enzyme molybdopterin synthase (Pitterle and Rajagopalan 1993). Mutations within *moeA* seem to have polar effects on MoeB production so it is thought that the two genes constitute a single transcriptional unit (Hasona *et al.* 1998). It should also be noted that the translational stop codon of *moeA* and the *moeB* start codon

overlap (Hasona *et al.* 1998). In the case of *P. furiosus* however, none of the *moeA* or *moeB* homologs appear to be located on a *moeAB* operon arrangement.

Expression studies show an increase in the expression of the *moe* operon when there is an increase in the production of the molybdoenzymes nitrate reductase and trimethylamine N-oxide (TMAO) reductase (Hasona *et al.*, 2001). Further results show transcription of the *moe* operon is physically coupled to increasing demand for the molybdenum cofactor, which the cell would encounter under conditions of nitrate respiration (Hasona *et al.*, 2001). However, it appears that the molybdenum status of the cell has no influence on *moeA* expression (Leimkühler *et al.*, 1999). Oxygen has been seen to have a negative effect on the *moe* expression. When a *moeA-lacZ* fusion strain was grown under aerobic and anaerobic conditions, there was a 2.5 fold increase in *moeA-lacZ* expression within the cells that were grown anaerobically (Hasona *et al.*, 2001).

Sequence similarity of *moeA* homologs can be seen in Bacteria, Archaea and eukaryotes, this conservation of protein sequence covers an evolutionary distance that is estimated to be at one billion years (Gallois *et al.* 1997). This conservation indicates the ancient origin of MoCo as well as the high evolutionary pressures present to maintain the genes that are involved in MoCo synthesis (Stallmeyer *et al.*, 1999). The eukaryotic proteins that exhibit sequence similarity are: cinnamon from the fruitfly *Drosophila melangaster*, *cnxE*, from the plant *Arabidopsis thaliana* (Stallmeyer *et al.* 1995), and gephyrin which is a mammalian neuroprotein characterized in rats that functions to link the mammalian inhibitory glycine receptor to subsynaptic microtubules (Prior *et al.* 1992). Many eukaryotic proteins contain two of the bacterial proteins needed for making the MoCo fused into a single peptide chain, however the orientation of the genes are not always the same within the

various organisms. For example in Cinnamon and gephyrin, the MogA like domain is at the N-terminus while the MoeA like domain is located in the C-terminal end (Stallmeyer *et al* 1995). Conversely, in the plant Cnx1 protein, the order is reversed, with the *E. coli* MogA-like domain at the C-terminus and the MoeA like domain at the N-terminus (Stallmeyer *et al* 1995). The gene domains that are fused together are separated by about 160 amino acids, this fusion domain has no homology to any other known protein (Stallmeyer *et al*, 1999).

The crystal structure of *E. coli* MoeA has been refined to 2 Å and reveals that the elongated L- shaped MoeA monomer consists of four separate domains (Schrag *et. al* 2001). Domains I and II form the upper portion, domain III forms the corner of the letter L and domain IV forms the base (Schrag *et. al* 2001). Domain I acts as a linker between domain II and III (Xiang, 2001). Domain III is structurally related to MogA, which is reportedly a molybdochelase responsible for the insertion of the Mo atom into molybdopterin to complete Moco synthesis (Schrag *et. al* 2001). This suggests that MoeA and MogA may bind similar ligands and therefore have similar functions (Schrag *et. al* 2001). In *E. coli*, the active form of MoeA is a dimer, and the putative active site seems to be localized to a cleft formed between the domain II of the first monomer and domains III and IV of the second monomer (Xiang, 2001).

Sequence alignments of MoeA proteins from different organisms reveal that there are a rather low number of strictly conserved residues (Xiang, 2001). These conserved residues seem to fall into two classes: those that are important to structure and those that are important to function (Xiang, 2001). The residues that appear to be structurally important are distributed throughout the entire molecule; they are the two *cis*-prolines and several residues within the hydrophobic core (Xiang, 2001). Conserved residues that may be important to

function of MoeA are Asp-59, Thr-100, and Asp-142 in domain II: Glu-188, Asn-205, and Asp 228 in domain III and Ser-371 in domain IV (Xiang, 2001). These residues are either grouped together at the cleft between domains III/IV and II or are located on a pocket on the surface of domain III (Xiang, 2001).

MoeB is the molybdopterin synthase sulfurase, the protein that is responsible for regenerating the thiocarboxylate group at the C terminus of MoeD in an ATP-dependent reaction (Rajagopalan 1997). There is experimental data that indicates MoeB itself is not sulfurated during the sulfur transfer reaction for the activation of MPT synthase and that its role is limited to generation of the acyl adenylate of MoeD (Leimkühler *et al* 2001). Mass spectrometry has shown a thiocarboxylate in the activated form of MoeD that serves as the sulfur donor for the synthesis of MPT to precursor Z (Pitterle *et al* 1993). There is data that strongly suggests that L-cysteine is most likely the physiological sulfur donor (Leimkühler *et al*, 2001). Organisms with mutations in the MoeB gene accumulate a sulfur free molecule of the precursor Z (Pitterle and Rajagopalan 1989).

E. coli MoeB is made up of 253 amino acids and has a calculated molecular mass of 26.6 kDa. *Rhodobacter capsulatus* MoeB has a high similarity, 41%, to ThiF from *E. coli* (Vander Horn *et al* 1993). It is thought that ThiF catalyzes the adenylation by ATP of the carboxyl-terminal glycine of ThiS, which is a reaction analogous to the adenylation of MoeD by MoeB. The ThiF reaction is likely to be involved in the activation of ThiS for sulfur transfer from cysteine or from a cysteine-derived sulfur donor (Taylor *et al* 1998). Upon experimentation it was observed that the Cys-184 residue of ThiF and the C terminus of ThiS thiocarboxylate were identified to be involved in the formation of ThiF/ThiS complex (Xi *et al* 2001).

A number of other proteins have also been identified as having significant sequence similarities to MoeB, one of these proteins is the eukaryotic ubiquitin-activating enzyme E1 which is encoded by *Uba1* (Rajagopalan 1997). Uba1 was shown to activate ubiquitin in an ATP dependant reaction with the initial formation of an Uba1-ubiquitin adenylate complex. This reaction is followed by generation of a thioester linkage between the C-terminal glycine of ubiquitin and cysteine residue of Uba1 (Varshavsky A 1997). Another protein with high similarity to *E.coli* MoeB is the eukaryotic CnxF from *Aspergillus nidulans*. It consists of 560 amino acid residues, which is considerably larger than the 253 amino acid *E.coli* MoeB. The increase in length is at both the C and N termini, unfortunately the function of the additional residues is still unknown (Appleyard *et al*, 1998).

MoeB contains several conserved cysteine residues. It has been reported in previous studies that mutations of residue Cys-263 in the MoeB equivalent CnxF in *Aspergillus nidulans* resulted in a loss of function of the protein for MPT biosynthesis. (Appleyard *et al*, 1998). This residue is currently a strong candidate for thioester formation between the synthase and the sulfurylase (Appleyard *et al*, 1998). In order to determine which residues were necessary for the formation of the putative thioester linkage with MoaD, Leimkühler *et al.* used site-directed mutagenesis to replace each of the cysteine residues with an alanine. When looking at the site directed mutagenesis in *E. coli moeB*, four of the mutants had decreased amounts of MPT. They were: C172A, C175A, C244A and C247A (Leimkühler *et al*, 1999). All of these residues are present in highly conserved Zn-binding motifs (Leimkühler *et al*, 1999). The exact role of the Zn within the MoeB protein is not known but it is thought to be involved in structural stabilization of the protein but not in the enzyme catalysis (Leimkühler *et al*, 1999).

Molybdenum and tungsten are chemically analogous elements, which perform essential roles in biology as components of enzyme cofactors (Kletzin and Adams 1996). As opposed to the molybdenum cofactor MoCo synthesis, which has been almost completely determined in mesophilic bacteria such as *Escherichia coli* and *Rhodobacter capsulatus*, the nature of tungsten cofactor synthesis remains undetermined. Since tungsten is obligately required for growth and tungstoenzymes are a key to certain reactions involved in central carbon metabolism, investigation of tungsten cofactor synthesis is important to understanding the physiology of hyperthermophilic Archaea such as *P. furiosus*. Furthermore there is no tungsten homolog for *modE* in *P. furiosus*, the regulator for molybdenum uptake and processing, so studies of the expression of tungsten cofactor synthesis will potentially provide valuable information in regards to tungsten metabolism and its regulation.

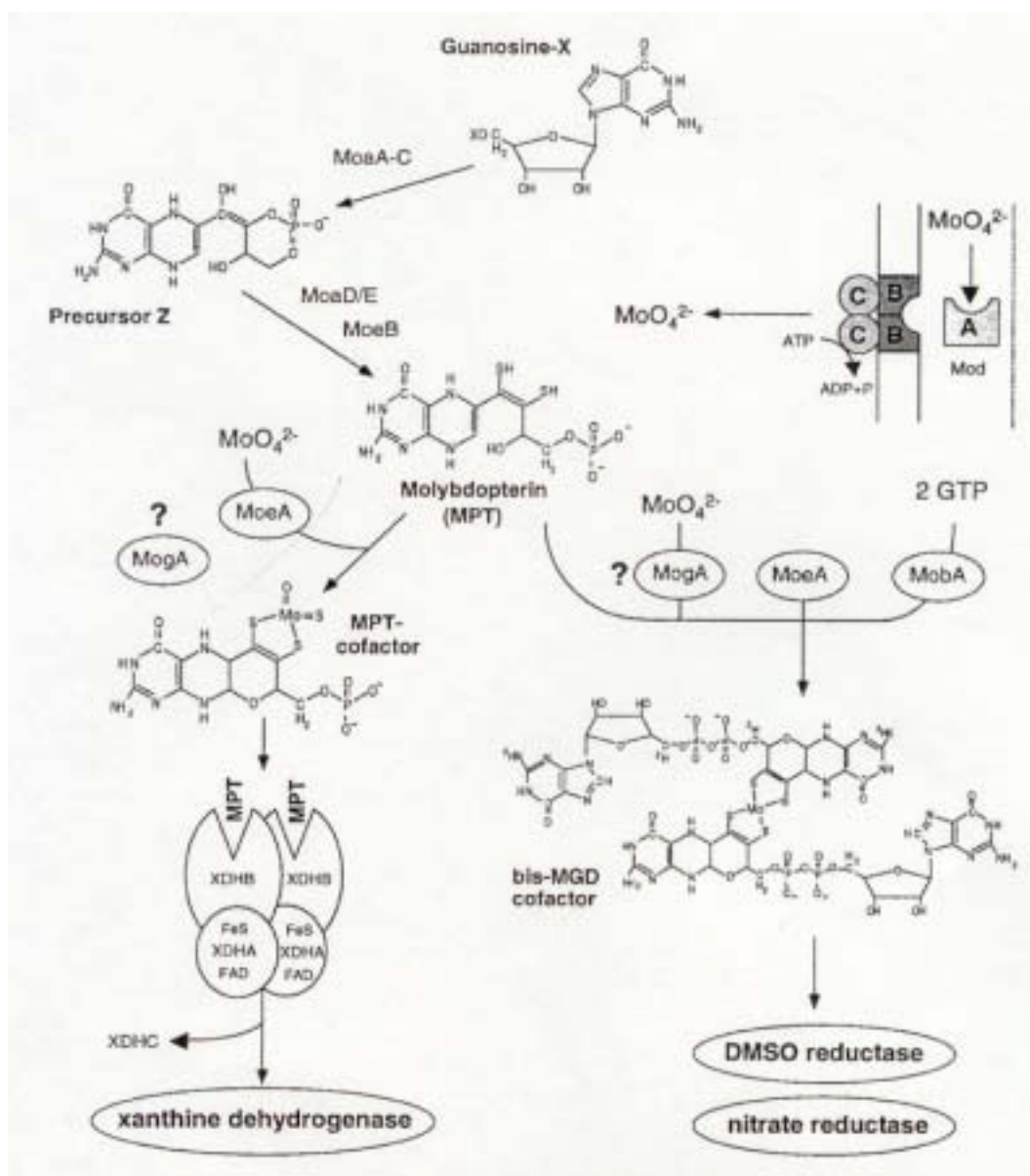


Figure 1: Molybdenum Cofactor Synthesis in the mesophilic bacterium *Rhodobacter capsulatus*. Modified from Leimkühlen, *et al* 1999

Table 1: *P. furiosus* molybdenum cofactor homologs

<i>P. furiosus</i> Genome Identifier #	MoCo Biosynthesis Homolog	MoCo Biosynthesis Gene Function	% Similarity to Known MoCo Biosynthesis Gene/Organism Source
PF97550	MoaA	Precursor Z synthesis	51%/E. coli
PF387554	MoaB	Precursor Z synthesis	52%/E. coli
PF1711292	MoaC	Precursor Z synthesis	63%/E. coli
PF258122	MoaD	Molybdopterin synthase	41%/E. coli
PF526899	MoaD (2)	Molybdopterin synthase	52%/E. coli
PF107582	MoaE	Molybdopterin synthase	52%/E. coli
PF162662	ModB	Molybdenum transport	50%/E. coli
PF9230	MoeB (2)	Sulfation of MPT	50%/Arabidopsis Thaliana
PF562615	MoeA	Activation of Mo	45%/E. coli
PF1657497	MoeA (2)	Activation of Mo	44%/E. coli
PF637268	MobA	MPT guanine dinucleotide synthase	51%/E. coli
PF1805554	MobB	GTP-binding protein	47%/Staphylococcus carneus
PF1216166	MoeB	Sulfurylation of MPT	44%/S. Carnosus

Materials and methods

Bacterial strains and plasmids. The bacterial strains and plasmids used in this study are presented in Table 2.

Construction of recombinant *P. furiosus moeA*, *moeA2*, and *moeB* expression plasmids.

P. furiosus moeA, *moeA2* and *moeB* genes were obtained by PCR amplification using *P. furiosus* template DNA and gene-specific primers with engineered *XhoI* and *EcoRI* restriction sites in the forward and reverse primers, respectively. The PCR amplification was performed using *P. furiosus* DNA polymerase, which has proofreading activity, and a Icyclcr (BioRad, Hercules, CA) programmed for 39 cycles with each cycle consisting of denaturation for 0.5 min. at 95 °C, annealing at 55 °C for 0.5 min, and extension at 72 °C for 2 min. The resulting PCR products (*moeA* gene 1301bp, *moeA2* gene 1271bp and *moeB* gene 751bp) were purified using the Qiaquick PCR purification kit (Qiagen, Valencia, CA) and digested with the restriction enzymes *XhoI* and *EcoRI* for cloning into the appropriate *XhoI/EcoRI* digested pBAD/His vector (Invitrogen, Carlsbad, CA). Vectors pBAD His A, B or C were chosen for each construct to provide His-tag for each recombinant protein. The resulting plasmids were designated pELM1 (*P. furiosus moeA* in pBAD hisA vector), pELM2 (*P. furiosus moeB* in pBAD hisB vector) and pELM3 (*P. furiosus moeA2* in pBAD his C) and were transformed into *E. coli* strains Top10 (pORF9230, and pELM3) or LMG194 (pELM1, and pELM2) for protein expression. The gene sequence for each of the expression plasmids was determined to ensure that no mutations were present in the expression clones (Molecular Genetics Information Facilities, University of Georgia, Athens, GA).

Expression and purification of recombinant His-tagged *P. furiosus MoeA*, *MoeA2*, *MoeB*, and *MoeB2* proteins. Expression of *MoeB2* is controlled by a T7 promoter with

high-level induction of recombinant His-tagged protein production in response to the presence of IPTG in the growth media. For initial optimization of recombinant protein production, 30 mL cultures of Top10/pORF9230 were grown in LB. The cultures were incubated at 37 °C with shaking. Once an optical density of 0.6 was reached, various concentrations of IPTG were added. Expression of proteins using the pBAD/His vectors is controlled by the *E. coli araBAD* promoter with high-level induction of recombinant N-terminal His-tagged protein production in response to the presence of L-arabinose in the growth media. For initial optimization of recombinant protein production, 30 mL cultures of Top10/pELM3 were grown in LB and LMG194/pELM2 and LMG194/pELM1 was grown in RM media (M9 media with 0.2% glucose, 2% casamino acids and 1mM MgCl₂). The cultures were incubated at 37 °C with shaking. Once an optical density of 0.6 was reached, various concentrations of L-arabinose were added (0.002% -2%). Protein expression was monitored using visual detection of Coomassie-stained 12.5% polyacrylamide gels and by Western detection using antibody specific for the His-tag. Based on the optimization experiments, the following conditions were used for 1 L expressions: MoeB2 was produced in Top10/pORF9230 cultures in LB at 37 °C with shaking to an OD of 0.6. IPTG was then added (400 µM final concentration) and the cultures incubated at 37°C for 4 hours before harvesting the cells. MoeA2 was produced in Top10/pELM3 cultures in LB at 37 °C with shaking to an OD of 0.6. L-arabinose was then added (0.2%) and the cultures incubated at 37°C for 4 hours before harvesting the cells. MoeA and MoeB were produced from LMG194/pELM1 and LMG194/pELM2 cultures, respectively, was grown up in RM media at 37 °C with shaking until an OD of 0.6. L-arabinose was then added to have a final

concentration of 0.2% and the culture incubated at 25°C with shaking for 8 hours before harvesting the cells

Pellets from one-liter expressions were resuspended in buffer (20 mM NaPO₄, 1 mM benzamidine-HCl, pH 7.2) and the cells broken by two passages through a French press (20,000 lb/in²). A cleared supernatant was prepared by spinning the broken cell suspension at 10,000 RPM for 20 minutes at 4°C. Contaminating *E. coli* proteins were initially removed from the protein extracts by incubating the extracts at 80 °C for 20 minutes and pelleting the denatured protein. The heat-treated protein solution was then applied to a 1 mL Hi-trapTM chelating HP column (Amersham Biosciences, Piscataway, NJ) in binding buffer (20 mM NaPO₄, 50 mM NaCl, 1mM DTT, pH 7.4) at a flow rate of 1ml/min. The Hi-trap chelating column preferentially binds His-tagged proteins. Bound protein was eluted in elution buffer (20 mM NaPO₄, 0.5 M NaCl, 0.5 M imidazole, 1mM DTT, pH 7.4). Eluted fractions containing recombinant protein were visually inspected for purity using Coomassie-stained 12.5% polyacrylamide gels. Pure fractions were combined and dialyzed into buffer (50 mM Tris-HCl, 1mM DTT, pH 8) to remove the imidazole. The proteins are then concentrated to ~ 0.14 mg/ml (MoeA), 0.4 mg/ml (MoeB), 5.0 mg/mL (MoeB2) and 2.79 mg/ml (MoeA2) and frozen at –80 °C in 50 µL aliquots.

***In vivo moeA and moeB* complementation assays based on *E.coli* nitrate reductase activity.** The ability of *P. furiosus* MoeA and MoeB homologs to complement *E. coli* strains deficient in MoeA (AH69 and AH215) and MoeB (AH30) production was examined by assaying for nitrate reductase activities, where restoration of nitrate reductase activity indicates complementation of the defects in molybdenum cofactor synthesis. For the *in vivo* complementation assays, *P. furiosus* MoeA, MoeA2 and MoeB expression plasmids were

transformed into the *E. coli moeB* (AH30) and *moeA* (AH69 and AH215) mutant strains. The transformants were grown aerobically over night in LB plus 0.3% glucose. The overnight cultures were used to inoculate 30 ml of LB media (0.05 % inoculum) that contained L-arabinose (0.2%), NaNO₃ (30 mM), molybdenum (50 μM) and ampicillin (100 μg/mL). These cultures were grown anaerobically for 4 hours and the harvested cells broken by passage through the French press (20,000 lb/in²). The broken cells were spun down and the resulting protein extract was placed in stoppered tubes and put under argon gas. Nitrate reductase activities were determined using a nitrite colorimetric determination method (Nicholas, 1957) where the reaction mixes contained in a 0.5 mL total volume: 0.1 mL 50 mM NaNO₃, 0.1 M NaKPO₄, 0.07 mL 1mM benzyl viologen, 50 μL protein extract for the mutant stains and 5 μL for the wild type extract, 0.05 mL 20 mM sodium dithionate. The mixtures were incubated for 5 minutes at room temperature before adding 0.5 mL 1% sulfanilic acid (in 20% HCL) and 0.5 mL 0.02% N-1(naphthyl-ethylene) diamine HCL. The solutions were allowed to develop at room temperature for 10 minutes. The solutions were diluted with 2 mL of dH₂O. 1.5 mL of the diluted mixture was spun at 15,000 rpm for 5 minutes and the absorbance of the supernatant was read at 540 nm.

***In vivo moeA and moeB* complementation assays based on TMAO reductase activity.**

Complementation of defects in *E. coli moeA* and *moeB* by the *P. furiosus* homologs was also investigated by monitoring activity of the molybdoenzyme, trimethylamine oxide (TMAO) reductase. In this case, the complementation strains harboring the appropriate *P. furiosus* expression plasmid (5 % inoculum) were cultured in 30 mL of LB supplemented with 20 mM TMAO, 0.2% glucose, 0.2% L-arabinose, and 50 μM of either molybdenum or tungsten. The cultures were grown anaerobically for 4 hours at 37 °C before harvesting the cells. The

pelleted cells were washed twice with buffer (0.1 M KPO₄ pH 7.3, 0.5 mM EDTA, 1.08 μM 2-mercaptoethanol, 1 mM benzamidine. Cells were frozen at -80° C for 20 minutes and then resuspended in 500 μL of wash buffer. The cell suspension was transferred to stoppered test tubes and placed under argon gas. TMAO reductase activity was measured spectrophotometrically at 37 °C by following the oxidation of reduced benzyl viologen at 600 nm coupled to the reduction of TMAO. All solutions required for the assay were made anaerobic prior to use. For the assay, varying amounts of freeze-thawed cell suspension (50 μL to 300 μL) were added to 1.4 mL of 50 mM sodium succinate, pH 6, 200 μL of sodium dithionate (20 mM) and 280 μL of benzyl viologen (1mM) in stoppered anaerobic cuvettes. The cuvettes were placed in the spectrophotometer chamber for 2 min. to reach 37 °C before initiating the reaction with the addition of 30 μl of 1 M TMAO.

***In vitro moeA and moeB* complementation assays**

Protein extracts of *E. coli moeB* (AH30) and *moeA* (AH69 and AH215) mutant strains were prepared from 1 L cultures grown anaerobically for 4 h. at 37 °C in LB media supplemented with glucose (0.3%), NaNO₃ (30 mM) and molybdenum (50 μM). Harvested cells were broken by passage through a French press (20,000 lb/in²) and the extract recovered after centrifugation at 10,000 RPM for 20 min. The resulting extract was transferred to stoppered test tubes and placed under argon gas. The *in vitro* complementation assay was based on the method developed by Adnan Hasona (personal communication) and involved the following steps: the complementation mix which consisted of: 5 μL 1 M NaKPO₄ pH 7.0, 2.5 μL 100 mM ATP, 5 μL 1 mg/mL BSA, 1 mM molybdenum, varying amounts of protein, and water to have a final volume of 50 μL was placed in stoppered test tubes and made anaerobic. 200

μL of the protein extract was then added to the complementation mix and incubated at 37°C for 1 hour. 50 μL of this mix was added to the assay mix described in the *in vivo* section. Successful complementation of either *E. coli* MoeA or MoeB with the *P. furiosus* homologs was determined using either nitrate reductase or TMAO reductase activity assays as indicated for the *in vivo* complementation methods.

Culturing *P. furiosus* in media with varying tungsten concentrations *Pyrococcus furiosus*

media was made in two steps. The base media which consisted of: 5X salts (NaCl, $\text{MgSO}_4 \cdot 6\text{H}_2\text{O}$, $\text{MgCl}_2 \cdot 6\text{H}_2\text{O}$, KCl, NH_4Cl and $\text{CaCl}_2 \cdot 2\text{H}_2\text{O}$) 1000X trace minerals (HCl, Na_4EDTA , FeCl_3 , H_3BO_3 , ZnCl_2 , $\text{CuCl}_2 \cdot 2\text{H}_2\text{O}$, $\text{MnCl}_2 \cdot 4\text{H}_2\text{O}$, $(\text{NH}_4)_2\text{MoO}_4$, $\text{AlK}(\text{SO}_4) 2\text{H}_2\text{O}$, $\text{CoCl}_2 \cdot 6\text{H}_2\text{O}$, $\text{NiCl}_2 \cdot 6\text{H}_2\text{O}$) resazurin and water was made in one liter batches. The media was placed in the hood and the cysteine HCl, Na_2S and NaHCO_3 was added, and the media was adjusted to a final pH of 6.8. The media was filter sterilized and was measured out into 40 ml or 400 ml aliquots in 100 mL or 1L stoppered serum bottles, respectively. The bottles were put on the manifold to degas and put under argon. The second step in making the *P. furiosus* media involved adding 0.2 mL 10% yeast extract, 0.4 mL 50% maltose, 0.04 mL 1M K-P buffer and various amounts of tungsten with the final concentrations ranging from 100 pM to 1 mM. Once all the components were added to the base media steps were taken to ensure there is not residual oxygen in the media. First the bottles were put on the manifold to remove any oxygen that was introduced as various media components were added. Then the media is heated to 95°C for fifteen minutes to ensure that the media was reduced, next the media is then cooled to room temperature before the addition of the inoculum. Once the inoculum has been added the bottles are placed at room temperature for an additional fifteen minutes before they are placed at 95°C . Different tungsten amounts, ranging from 100 pM

tungsten to 1 mM tungsten, were used in the media to see if this variance had any effect on the expression of the cofactor synthesis genes. Cells were grown to mid log phase (16 hours) at 95°C. All of the cultures were started with a 1% inoculum from cells grown in 10 µM tungsten. Following the initial inoculum, all the cultures were started with a 1% inoculum from the cells grown the night before. There were 3 transfers of cells in 40 mL size cultures and then the final transfer into a 400 mL culture. Once this culture had reached mid log phase the media was quickly chilled by pumping the culture through an ice water-cooled glass cooling coil. Once all the media was cooled the cells were pelleted at 5,000 RPM, RNA was subsequently isolated from the harvested cells.

RNA isolation. After the cells were pelleted the supernatant was discarded, leaving about 100 µL to resuspend the cells. The MasterPure™ RNA Purification Kit (Epicentre Technologies, Madison, WI) was used with some modifications. For the lysis of the cell samples and the precipitation of the total RNA, the solutions were scaled up 8 times the amount to account for the large amount of cell matter. Since the isolated RNA was to be used for RT-PCR experiments, removal of DNA contamination was required. DNA removal was performed as per the manufacturers recommendations with the following modifications: the required solutions were doubled and the mix was incubated at 37 °C for one hour. The isolated RNA was resuspended in 50 µL TE buffer and quantified by using spectrophotometry and electrophoresed through a 1.8% agarose gel for a visual inspection of the quality.

Real time RT PCR. In order to quantify the copies of mRNA coding for the tungsten cofactor synthesis genes that was present in each of the RNA isolates, a standard curve was created. This was accomplished using the PCR amplification of known quantities of template

DNA. The template was diluted so there was a range of 10^3 to 10^9 copies per well. In addition to the DNA template the following components were added to the PCR mix: TAQ buffer, TAQ polymerase, DNTP, forward and reverse primers for MoeA2, magnesium chloride, SYBR® Green I, fluorescein and water to make 50 μ L. The reaction was run on an Icyler (BioRad, Hercules, CA) fitted with the real time optical unit programmed for 39 cycles with each cycle consisting of denaturation for 0.5 min. at 95 °C, annealing at 55 °C for 0.5 min, and extension at 72 °C for 1 min. A standard curve was derived from the standard plate data that was used to determine the amount of RNA present in the experimental RT-PCR reactions. The Qiagen™ OneStep RT-PCR kit was used to complete the experimental RT-PCR reactions; one μ g of RNA was added to each sample. The only modification made to the suggested protocol was the addition of SYBR® Green 1 and fluorescein for the detection of PCR products by fluorescence. RNA levels of the following genes: MoeA, MoeA2, MoeB, ModB, MoaD2, MoaC, MoaB and GAOPR were determined using RNA isolated with varying tungsten concentrations. The reactions were run on the same an Icyler (BioRad, Hercules, CA) as the standard plate but the program consisted of a 50 °C incubation for 30 min for the reverse transcriptase portion of the experiment and a 15 min incubation at 95 °C to initiate the HotStar DNA polymerase. Then the program continued for 39 cycles with each cycle consisting of denaturation for 0.5 min. at 95 °C, annealing at 55 °C for 0.5 min, and extension at 72 °C for 1 min. Initial mRNA copies were determined by comparing the exponential cycle threshold values to those obtained for the standards.

Table 2. Bacterial strains and plasmids used in this study

Strain ^a or Plasmid	Genotype	Source
Strains: TOP10	<i>F⁻ mcrA Δ(mrr-hsdRMS-mcrBC) φ80lacZΔM15 ΔlacX74 deoR recA1 araD139 Δ(araA-leu7696) galU galK rpsL endA1 nupG</i>	Invitrogen
LMG194	<i>F⁻ ΔlacX74 galE thi rpsL ΔphoA Δara174 leu::Tn10</i>	Invitrogen
BW25113	<i>lacI^f rrnB_{T14} ΔlacZ_{wj16} hsdR514 ΔaraBAD_{AH33} ΔrhaBAD_{LD78}</i>	Datsenko, 2000
BW545	<i>Δ(lacU)169 rpsL</i>	Lab collection
AH30	BW545 <i>moeB101-Km</i>	K. T. Shanmugam
AH69	BW545 <i>ΔmoeA113 Δzbi-Km</i>	K. T. Shanmugam
AH215	BW25113 <i>ΔmoeA</i>	K. T. Shanmugam
Plasmids: pBAD/His	<i>P_{BAD} araC Amp^r</i>	Invitrogen
pELM1	pBAD/His A <i>P. furiosus moeA</i>	This study
pELM4	pBAD His B <i>P. furiosus moeB</i>	This study
pELM3	pBAD His C <i>P. furiosus moeA2</i>	This study
pAH79	<i>P_{tac} E. coli moeB Amp^r</i>	K. T. Shanmugam
pORF9230	Invitrogen Topo plasmid with T7 promoter and His Tag <i>P. furiosus moeB2</i>	Michael Adams

^aAll listed strains are *E. coli* K12 derivatives.

Results

Construction of recombinant *P. furiosus moeA*, *moeA2*, and *moeB* expression

plasmids To determine which, if any, of the predicted *P. furiosus moeA* and *moeB* homologs are the true functional homologs, the *P. furiosus moeA*, *moeB* and *moeA2* genes were PCR amplified and cloned into pET 21b. Unfortunately there were a number of technical difficulties cloning the *P. furiosus moeA*, *moeB* and *moeA2* genes into the pET 21b vector. To overcome these problems the pBAD/His vector system was used. *P. furiosus moeA*, *moeB* and *moeA2* genes were PCR amplified and cloned into the appropriate pBAD/His vector. These plasmid constructs were named pELM1 for *P. furiosus MoeA*, pELM2 for *P. furiosus MoeB* and pELM3 for *P. furiosus MoeA2* and the gene sequences were verified by sequencing (MGIF, Athens, Georgia). All of the plasmid constructs were transformed into *E. coli* Top10 for expression. L-arabinose was added from 0.002%-2% to determine optimal expression. SDS –PAGE analysis was performed to determine the level of expression. These gels were transferred to nitrocellulose and His specific antiserum was used to detect level of expression. It was observed that the proteins were not over expressed well under any of the initial conditions. The lack of over expression was thought to be from an insufficient amount of rare codons being produced, which are necessary for protein expression. To overcome this problem a rare codon plasmid, PRIL, was transformed into each of the expression strains. Even after the PRIL plasmid was transformed into the expression strain with pELM1 and pELM2, the MoeA and MoeB protein respectively, did not express very well. One possibility was that the MoeA and MoeB proteins were toxic to the cells due to leaky expression. To address this possibility pELM1 and pELM2 were transformed into *E. coli* strain LMG194, which has tighter control over the expression of the plasmid. LMG194/pELM1 and

LMG184/pELM2 were grown in RM media at 37°C for 4 to 8 hours, 25°C for 12 hours and 4°C for 24 hours, but higher levels of protein expression was never achieved.

Purification of recombinant His-tagged *P. furiosus* MoeA, MoeA2, and MoeB proteins.

To purify the recombinant *P. furiosus* proteins, cells from each expression were lysed and then heat-treated to denature the majority of the *E. coli* proteins. The cell extracts were applied to a 1 mL Hi-trap™ chelating HP column, which preferentially binds His-tagged proteins. A chromatogram from the MoeA2 HPLC purification is shown in Figure 2. The blue line represents the UV trace that indicates the amount of protein eluting from the column. The first peak represents the protein that is not bound to the column (flow through) while the second smaller peak represents the protein that bound to the column and was eluted off with increasing concentration of elution buffer that is represented by the black line. Both MoeA2 and MoeB2 eluted off as distinct peaks. However, the MoeA and MoeB proteins eluted in broader shallower peaks, which based on coomassie stained gels contained only purified recombinant protein. The purified protein samples were concentrated and aliquots from the various steps of the purification were electrophoresed through a 12.5% polyacrylamide a gel to confirm the purity. The steps of the MoeA2 purification are presented in Figure 3 and the MoeB2 purification is shown in Figure 4. All of the final purified recombinant *P. furiosus* proteins used in this study are shown in Figure 5.

***In vivo moeA* complementation studies demonstrate that *P. furiosus moeA2* can functionally substitute for *E. coli moeA*.** The *in vivo* complementation assays have demonstrated in three separate experiments that *P. furiosus moeA2* is able to complement the

moeA deletion in *E. coli* strain AH215 (Table 3). The *in vivo* assay utilized the complementation strains harboring the appropriate *P. furiosus* expression plasmid and nitrate reductase activities were determined using a nitrite colorimetric determination method. The data indicate that *P. furiosus moeA2* is capable of supporting approximately one third the level of nitrate reductase activity as compared to the wild type *E. coli* strain, 50 nmole $\text{NO}_2^- \bullet \text{min}^{-1} \bullet \text{mg}^{-1}$ for *P. furiosus moeA2* compared to 152 nmole $\text{NO}_2^- \bullet \text{min}^{-1} \bullet \text{mg}^{-1}$ for wild type *E. coli* (Table 3). However, *P. furiosus moeA* did not appear able to complement for the *E. coli moeA* mutation, as only 1.18 nmole $\text{NO}_2^- \bullet \text{min}^{-1} \bullet \text{mg}^{-1}$ units of activity were obtained when *P. furiosus moeA* containing plasmid was introduced into *E. coli* AH215 (Table 3). However it must be noted that the *in vivo* experiments are essentially qualitative in nature. Meaning that data can be relied upon when complementation is observed, but that a negative result could be due to failure to express the protein rather than the inability of the recombinant protein to functionally substitute for the mutant. Since the *in vivo* assays can really only provide a more qualitative measure of potential complementation, *in vitro* assays were conducted in which known amounts of purified protein can be added to the assay in an effort to obtain more quantitative results.

***In vitro moeA* complementation assays also confirm that only *P. furiosus MoeA2* can functionally substitute for *E. coli MoeA*.** The *in vitro* assays utilized the *E. coli moeA* (AH69 and AH215) mutant strains and purified *P. furiosus MoeA* and *MoeA2* protein. Initial studies were completed with *E. coli* AH69; however, this strain exhibits residual activity in the absence of added functional *MoeA* due to the leaky nature of the mutation. This caused difficulty in accurately determining specific activities. In order to avoid these problems *E. coli*

strain AH215 was used in place of AH69. AH215 has a complete deletion of the *E. coli moeA* gene, and as a result much less background activity was observed using this strain. For the *in vitro* assays, the mutant strain cells were grown and various amounts of purified *E. coli* MoeA, *P. furiosus* MoeA or MoeA2 were added to the complementation mixtures. Since *P. furiosus* normally grows at 95 °C a short incubation time was added, before the 37 °C incubation, to determine if a higher temperature was needed for the *P. furiosus* proteins fold correctly. The temperatures used in the assays ranged from 37 °C to 90 °C, at 37 °C there was 11.3 nmole NO₂⁻•min⁻¹•mg⁻¹ at 60 °C there was 13.1 nmole NO₂⁻•min⁻¹•mg⁻¹ then there was a constant decrease in activity until at 90 °C where there was only 2.2 nmole NO₂⁻•min⁻¹•mg⁻¹. The incubation times ranged from 1 minute to 30 minutes, where the activity increased until the 10-minute time point where the activity began to drop off dramatically. Experiments demonstrated that the highest activity was when complementation mixes were exposed to 60 °C for 5 minutes (data not shown). The 100 µL of the heated mixture was combined with 100 µL of the non-heated mixture to insure that there were functioning *E. coli* proteins present during the one-hour incubation at 37 °C. As with the *in vivo* assays the nitrate reductase activities were calculated using a nitrite colorimetric determination method. The *in vitro* experiments concur with the *in vivo* assays, as both assays show that *P. furiosus* MoeA2 protein can restore nitrate reductase activity in the *E. coli moeA* deletion strain. The data from these experiments showed the maximum observed nitrate reductase activity for *P. furiosus* MoeA2 (13.1 nmole NO₂⁻•min⁻¹•mg⁻¹) is only about one tenth that seen for the wild type strain (130 nmole NO₂⁻•min⁻¹•mg⁻¹) (Figure 6). However the amount of activity observed for the complementation with *P. furiosus* MoeA2 is quite significant considering the purified *E. coli* MoeA had a maximum observed nitrate reductase activity of 17.3 nmole

$\text{NO}_2^- \cdot \text{min}^{-1} \cdot \text{mg}^{-1}$, which was only one seventh that seen for the wild type strain (Figure 6). Furthermore, the *in vitro* study shows that the complementation of *E. coli moeA* by *P. furiosus* MoeA2 can be achieved over a range of MoeA2 amounts with low levels of activity being detected when 50 ng of *P. furiosus* MoeA2 ($0.47 \text{ NO}_2^- \cdot \text{min}^{-1} \cdot \text{mg}^{-1}$) was added to the complementation mixture and maximum activity levels when 10 μg of MoeA2 ($13.1 \text{ NO}_2^- \cdot \text{min}^{-1} \cdot \text{mg}^{-1}$) was present (Figure 6). Also *E. coli* MoeA was able to complement over a range of MoeA amounts. The minimum level of activity was seen at 50 ng ($6 \text{ NO}_2^- \cdot \text{min}^{-1} \cdot \text{mg}^{-1}$) and maximum activity was seen at 10 μg ($17.3 \text{ NO}_2^- \cdot \text{min}^{-1} \cdot \text{mg}^{-1}$) (Figure 6) Unlike *E. coli* MoeA and *P. furiosus* MoeA2, the *P. furiosus* MoeA protein does not appear to complement the *E. coli moeA* deletion in either *in vivo* or *in vitro* assays (Table 3; Figure 6), and therefore its role in tungsten cofactor biosynthesis is in question.

The use of *in vivo* trimethyl amine oxide reductase assays to determine whether *P. furiosus* MoeA2 functionally discriminate between tungsten and molybdenum. In order to determine whether *P. furiosus* MoeA2 was preferentially functional with molybdenum as opposed to tungsten, TMAO complementation assays were used. TMAO assays were chosen to examine the role of the tungsten/molybdenum because it is the only known molybdoenzyme that is able to function with tungsten in place of molybdenum. Another potential advantage to using the TMAO reductase assays is that it could be assayed at high temperatures (80 °C) with tungsten. Unfortunately we could not take advantage of the higher temperatures because benzyl viologen oxidation occurred in a non-specific manner without the addition of TMAO when the higher temperatures were used (data not shown). Trial assays were done to determine the optimal temperature for the assays. It was observed that

the best activity was obtained at 37 °C. *In vivo* complementation assay using TMAO reductase activity utilized the complementation strains harboring the appropriate *P. furiosus* expression plasmid. Stopped anaerobic cuvettes were used to measure TMAO reductase activity spectrophotometrically at 37 °C by following the oxidation of reduced benzyl viologen at 600 nm coupled to the reduction of TMAO. Neither of the strains containing the *P. furiosus* MoeA or MoeA2 plasmids showed dramatic activity (data not shown). It was thought the lack of TMAO activity might have resulted from poor *P. furiosus moeA* or *moeA2* expression within the cells. These inconclusive results prompted further analysis of *moeA* complementation using the *in vitro* complementation assay system.

***In vitro* complementation assays using molybdenum-based and tungsten-based TMAO reductase activity has demonstrated that *P. furiosus* MoeA2 is able to complement the *moeA* deletion in *E. coli* strain AH215.** In this case, the mutant strain extract was added to a complementation mixture that contained purified *P. furiosus* MoeA2. Including *P. furiosus* MoeA in the TMAO assays was unfeasible, due to the small yield of protein from the *P. furiosus* MoeA purifications too much volume would have to be added to the complementation mixes to obtain a sufficient amount of protein. Unfortunately from this lack of data we cannot rule out the possibility that *P. furiosus* MoeA could substitute functionally for *E. coli* MoeA when a tungsten cofactor is synthesized, and further investigation of this possibility still needs to be completed. TMAO reductase activity was measured spectrophotometrically at 37 °C by following the oxidation of reduced benzyl viologen at 600 nm coupled to the reduction of TMAO. The *in vitro* assay data indicate that *P. furiosus moeA2* is capable of supporting approximately one sixtieth of the level of TMAO reductase

activity as compared to the wild type *E. coli* strain, 40.97 nmole TMAO reduced $\cdot\text{min}^{-1}\cdot\text{mg}^{-1}$ and 2,374.85 nmole TMAO reduced $\cdot\text{min}^{-1}\cdot\text{mg}^{-1}$ respectively (Figure 7). Furthermore, when molybdenum is used in the growth media the *in vitro* TMAO assays shows that the complementation of *E. coli moeA* by *P. furiosus* MoeA2 can be achieved over a range of MoeA2 amounts with low levels of activity being detected when 500 ng of *P. furiosus* MoeA2 was added to the complementation mixture and maximum activity levels when 10 μg of MoeA2 was present (Figure 7). However, when tungsten is used in the growth media there is a lower level of activity being detected with both the *E. coli* wild type strain as well as with AH215 complemented with the *P. furiosus* MoeA2. Because both of the strains have lower activity the data indicate that *P. furiosus* MoeA2 is capable of supporting approximately one six hundredth of the level of TMAO reductase activity as compared to the wild type *E. coli* strain, 2.07 nmole TMAO reduced $\cdot\text{min}^{-1}\cdot\text{mg}^{-1}$ and 1,297 nmole TMAO reduced $\cdot\text{min}^{-1}\cdot\text{mg}^{-1}$ respectively (Figure 8). These results indicate under these assay conditions, *P. furiosus* MoeA2 does not appear to functionally substitute for *E. coli* MoeA to a greater extent in the presence of tungsten rather than molybdenum.

***In vitro moeB* complementation assays confirm that *P. furiosus* MoeB2 can functionally substitute for *E. coli* MoeB.** For the *in vitro* assays AH30 cell extract was added to the complementation mixture containing *P. furiosus* MoeB2 and nitrate reductase activities were determined using a nitrite colorimetric determination method. Figure 9 shows that *P. furiosus* MoeB2 can complement the *E. coli moeB* mutation over a range of MoeB2 amounts and compare favorably with activity levels observed when *E. coli* MoeB is used (24 nmole $\text{NO}_2^- \cdot\text{min}^{-1}\cdot\text{mg}^{-1}$). Low levels of activity were detected when 10 μg of *P. furiosus* MoeB2 (6.4

nmole $\text{NO}_2^- \cdot \text{min}^{-1} \cdot \text{mg}^{-1}$) was added to the complementation mixture and maximum activity levels when 100 μg of MoeB2 was present ($19.6 \text{ nmole NO}_2^- \cdot \text{min}^{-1} \cdot \text{mg}^{-1}$). The same experiments were repeated using *P. furiosus* MoeB and only negligible nitrate reductase activity was observed ($0.74 \text{ nmole NO}_2^- \cdot \text{min}^{-1} \cdot \text{mg}^{-1}$). These nitrate reductase-based *in vitro* *E. coli* MoeB complementation assays indicate that *P. furiosus* MoeB2 can functionally substitute for *E. coli* MoeB while *P. furiosus* MoeB does not appear to do so.

***In vitro* moeB complementation assays based on TMAO reductase activity** *In vitro*

complementation assays using molybdenum-based TMAO reductase activity has demonstrated that *P. furiosus* MoeB2 is able to complement the *moeB* deletion in *E. coli* strain AH30. In this case AH30 protein extract was added to a complementation mixture that contained purified *P. furiosus* MoeB2. Stopped anaerobic cuvettes were used to measure TMAO reductase activity spectrophotometrically at 37 °C by following the oxidation of reduced benzyl viologen at 600 nm coupled to the reduction of TMAO. The *in vitro* assay with molybdenum data indicate that *P. furiosus* MoeB2 is capable of supporting approximately one four hundredth the level of TMAO reductase activity as compared to the wild type *E. coli* strain, $6.33 \text{ nmole TMAO reduced} \cdot \text{min}^{-1} \cdot \text{mg}^{-1}$ and $2,731 \text{ nmole TMAO reduced} \cdot \text{min}^{-1} \cdot \text{mg}^{-1}$ respectively (Table 6). As it can be seen in Figure 10, MoeB2 can complement for the *E. coli moeB* mutation over a range of protein amounts. When the cells were grown in media containing molybdenum the amounts of MoeB2 necessary for activity was $1 \mu\text{g}$ and the maximum activity was seen at $10 \mu\text{g}$. However, with tungsten present the *in vitro* assay data indicate that *P. furiosus* BoeB2 is capable of supporting approximately one two hundredth the level of TMAO reductase activity as compared to the wild type *E. coli*

strain, 6.0 nmole TMAO reduced•min⁻¹•mg⁻¹ and 1297 nmole TMAO reduced•min⁻¹•mg⁻¹ respectively (Table 7). The *in vitro* assay with tungsten data indicate that the level of MoeB2 necessary for activity was seen at 10μg and maximum activity was seen at 100μg (Figure 11). Therefore, it does not appear that *P. furiosus* MoeB2 functions more efficiently when a tungsten cofactor is synthesized versus a molybdenum cofactor. Including *P. furiosus* MoeB in the TMAO assays was unfeasible. Due to the small yield of protein from the *P. furiosus* MoeB purifications too much volume would have to be added to the complementation mixes to obtain a sufficient amount of protein. Unfortunately from this lack of data we cannot rule out the possibility that *P. furiosus* MoeB could substitute functionally for *E. coli* MoeB when a tungsten cofactor is synthesized.

Real time RT PCR. To begin to understand how the tungsten cofactor synthesis is regulated in *P. furiosus*, real time RT PCR experiments were completed. These experiments looked at the amount of mRNA produced which encodes various tungsten cofactor synthesis genes, when various amounts of tungsten were added to the *P. furiosus* growth media. In order to be able to quantify how much mRNA was present in the reactions, a standard curve was developed. This was completed by using known quantities of DNA and determining how long it takes the DNA to amplify exponentially, which is represented by the SYBR® Green I, and fluorescein being visualized by the real time optical unit. Figure 12 shows the standard curve, which was used to determine the amount of mRNA that was present for the genes involved in tungsten cofactor synthesis within the various tungsten growth studies. mRNA isolated from cells grown with a specific amount of tungsten was mixed with the reagents from the Qiagen™ OneStep RT-PCR kit. This mix was added to wells that contained

primers for some of the genes necessary for tungsten cofactor synthesis. The real time RT-PCR program generated two graphs. The first graph indicated the threshold cycle, this is the point at which the amount of cDNA exceeds an arbitrary limit determined by fluorescence detection (Figure 13). The second graph indicates the melting point of each of the products formed. This helps distinguish if products were real products, which have melting points around 90°C, or if they were primer dimers, which have melting points about 70 °C (Figure 14). Once the average threshold values were determined (Table 8) the standard curve was used to find the initial copy number of mRNA present in each reaction (Tables 9). Figure 15 represents the fold difference of tungsten cofactor synthesis gene expression levels in response to varying amounts of tungsten in the growth media. The mRNA obtained from each growth condition was compared to the mRNA isolated from cells grown in 10µM tungsten, which is the standard quantity present in *P. furiosus* growth media. A one-fold difference means there was the same amount of mRNA found in both of the growth conditions. The only gene that has a significant difference is Moad2. It has a 4 fold decrease with 100 pM and 1 nM, a 2 fold decrease with 100 nM and a 16 fold decrease with 1 mM tungsten. It is difficult to say at this time what is causing this decrease in mRNA production with out doing additional studies.

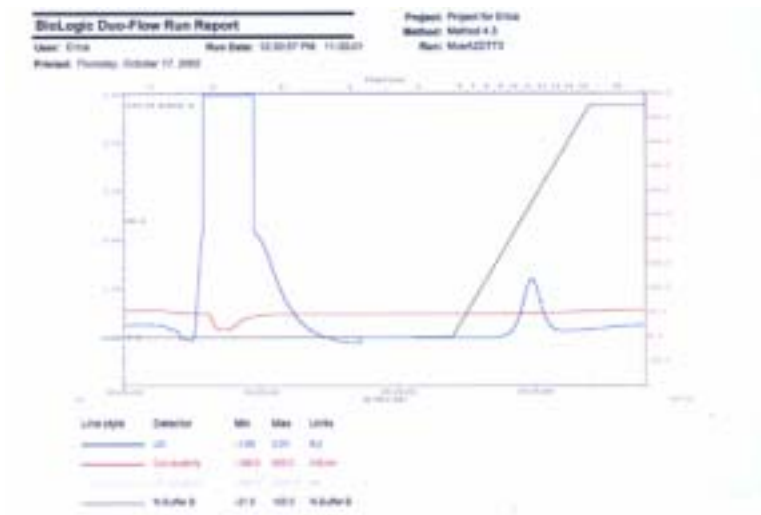


Figure 2: Representative chromatogram illustrating elution of recombinant *P. furiosus* MoeA2 from the metal chelation column. The blue line represents the UV trace. The first peak is the protein that is not binding to the metal chelation column (flow through). The second smaller peak is the *P. furiosus* MoeA2 which has bound to the column but has come off with the increasing concentration of elution buffer which is shown by the black line.

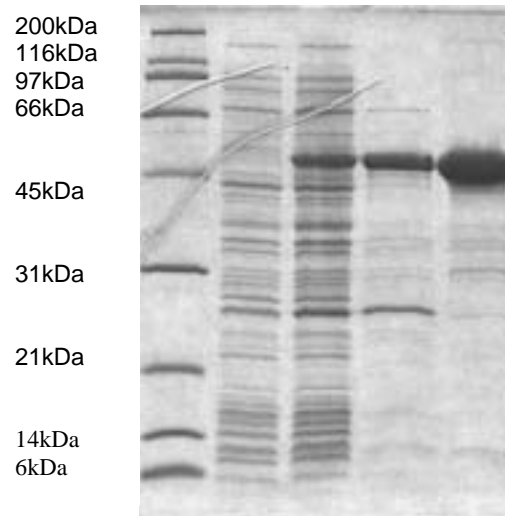


Figure 3: *P. furiosus* MoeA2 purification protein gel. Lane 1: MW standard, Lane 2: Uninduced cell extract, Lane 3: Induced cell extract, Lane 4: Heat treated extract, Lane 5: MoeA2 eluted from metal chelation column. Approximately 1 μ L of protein was added into each lane.

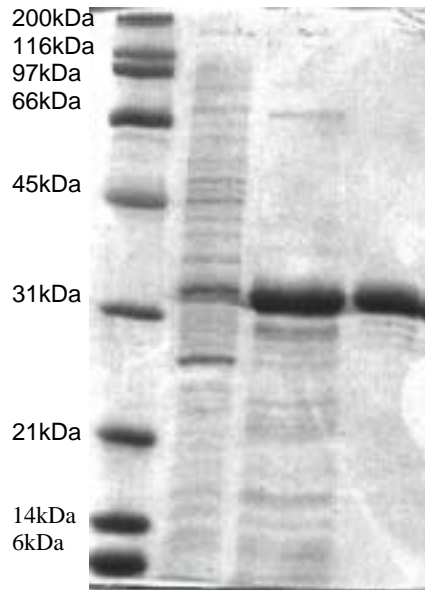


Figure 4. *P. furiosus* MoeB2 purification protein gel. Lane 1: MW standard, Lane 2: Whole cell extract, Lane 3: Heat treated extract, Lane 4: MoeB2 eluted from metal chelation column. Approximately 1 μ L of protein was added into each lane.

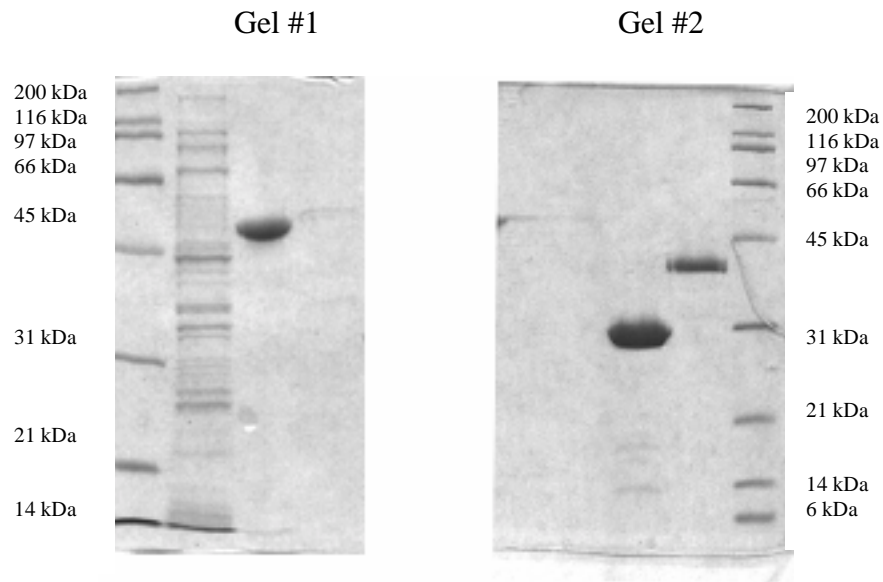


Figure 5: Purified recombinant *P. furiosus* MoeA2, MoeA, MoeB2 and MoeB proteins used in this study. Gel #1 Lane 1 MW standard, Lane 2 Whole cell extract, Lane 3 Purified *P. furiosus* MoeA2, Lane 4 Purified *P. furiosus* MoeA Gel #2 Lane1 *P. furiosus* MoeB2, Lane 2 *P. furiosus* MoeB, Lane3 MW standard. Approximately 1 μ L of protein was added into each lane except for the purified *P. furiosus* MoeA and purified *P. furiosus* MoeB that contain approximately 0.4 and 0.7 μ L of protein respectively.

Nitrate reductase activity versus *P. furiosus* MoeA2 and MoeA amount

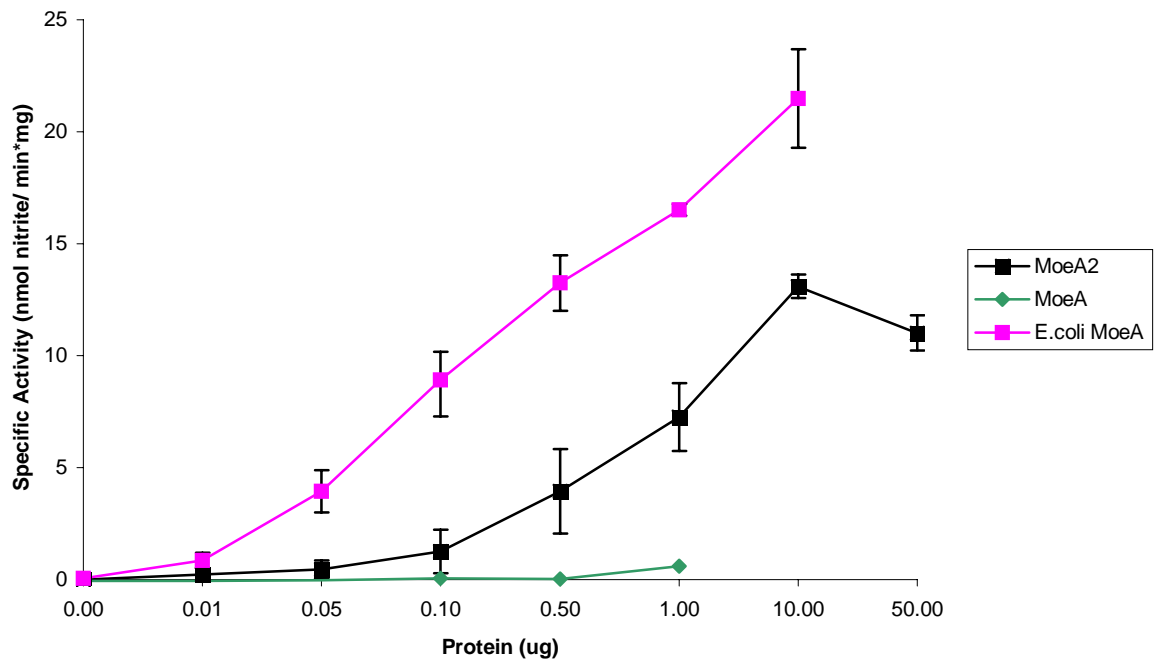


Figure 6: *In vitro* complementation of *E.coli moeA* mutation with *P. furiosus* MoeA, MoeA2 and *E.coli* MoeA detected using nitrate reductase assays. Specific activities were calculated using a nitrite colorimetric determination method. The error bars represent the differences between the three experiments.

TMAO reductase activity verses *P. furiosus*MoeA2 amount

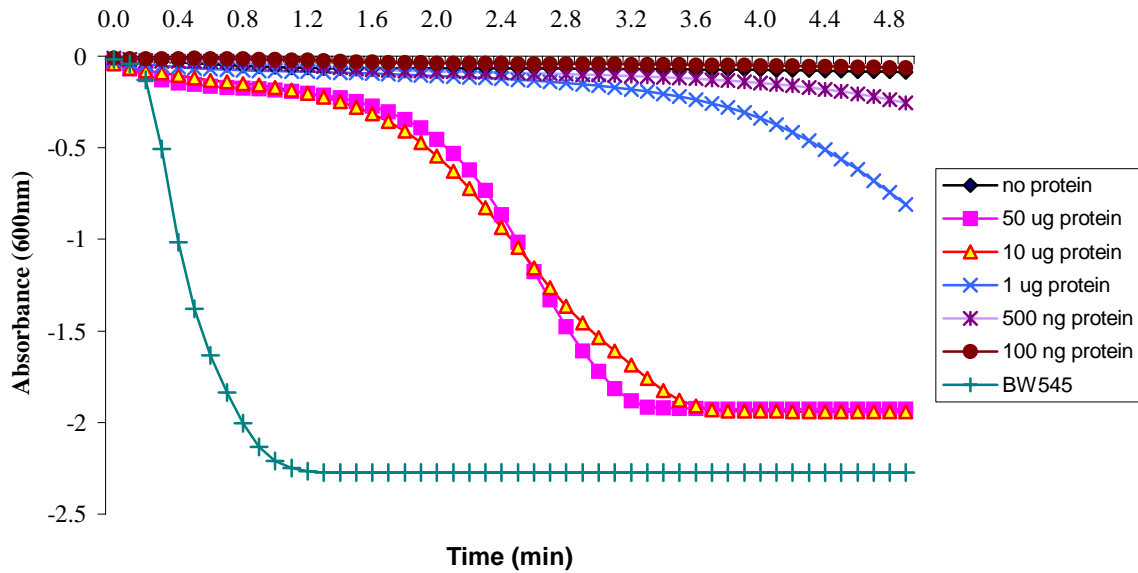


Figure 7: *In vitro* complementation of *E.coli moeA* mutation with *P. furiosus* MoeA2 detected with TMAO reductase assays. *E.coli moeA* mutant cells were grown in the presence of molybdenum. Specific activities were determined by the measuring the oxidation of reduced benzyl viologen at 600 nm coupled to the reduction of TMAO.

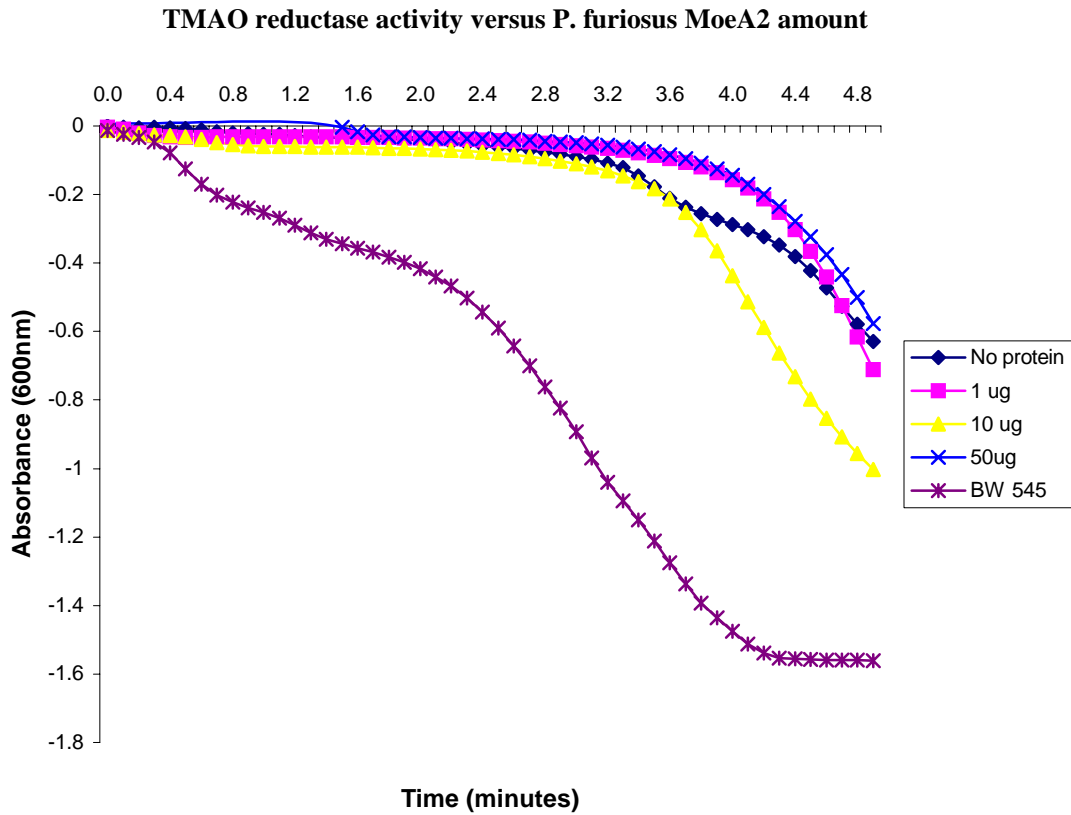


Figure 8: *In vitro* complementation of *E.coli moeA* mutation with *P. furiosus* MoeA2 detected with TMAO reductase assays. *E.coli moeA* mutant cells were grown in the presence of tungsten. Specific activities were determined by the measuring the oxidation of reduced benzyl viologen at 600 nm coupled to the reduction of TMAO.

Nitrate reductase activity versus *P. furiosus* MoeB, MoeB2 and *E.coli* ThiF amount

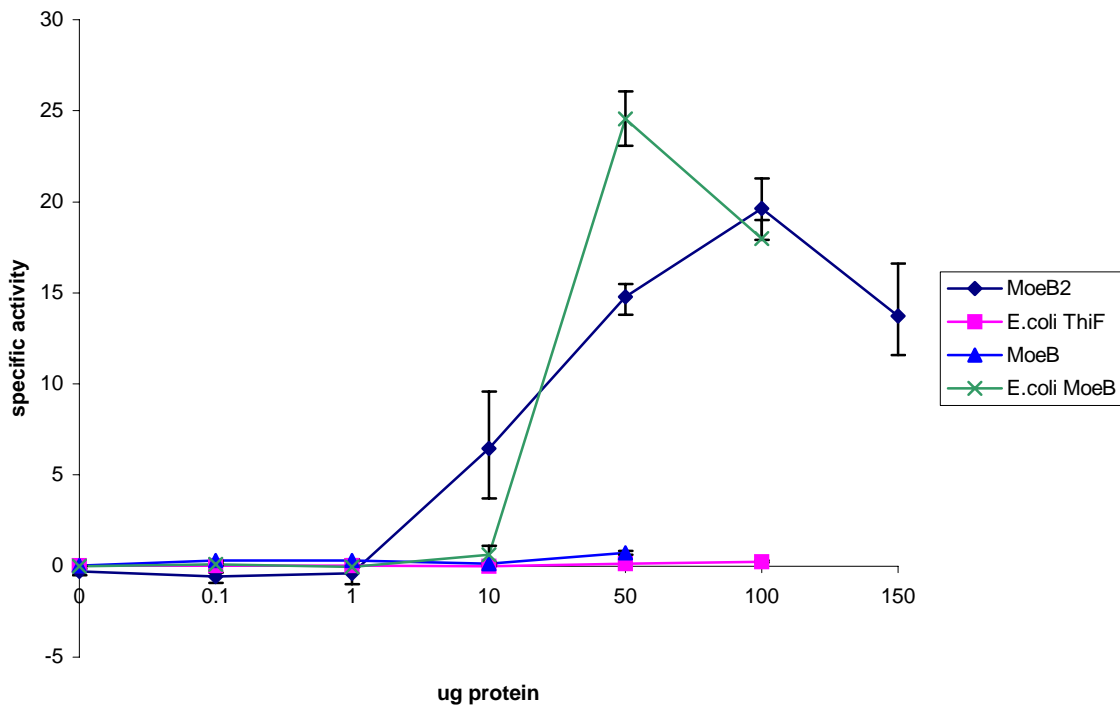


Figure 9: *In vitro* complementation of the *E.coli moeB* mutation with *P. furiosus* MoeB, MoeB2, *E.coli* MoeB and *E. coli* ThiF detected using nitrate reductase assays. Specific activities were determined using a nitrite colorimetric determination method.

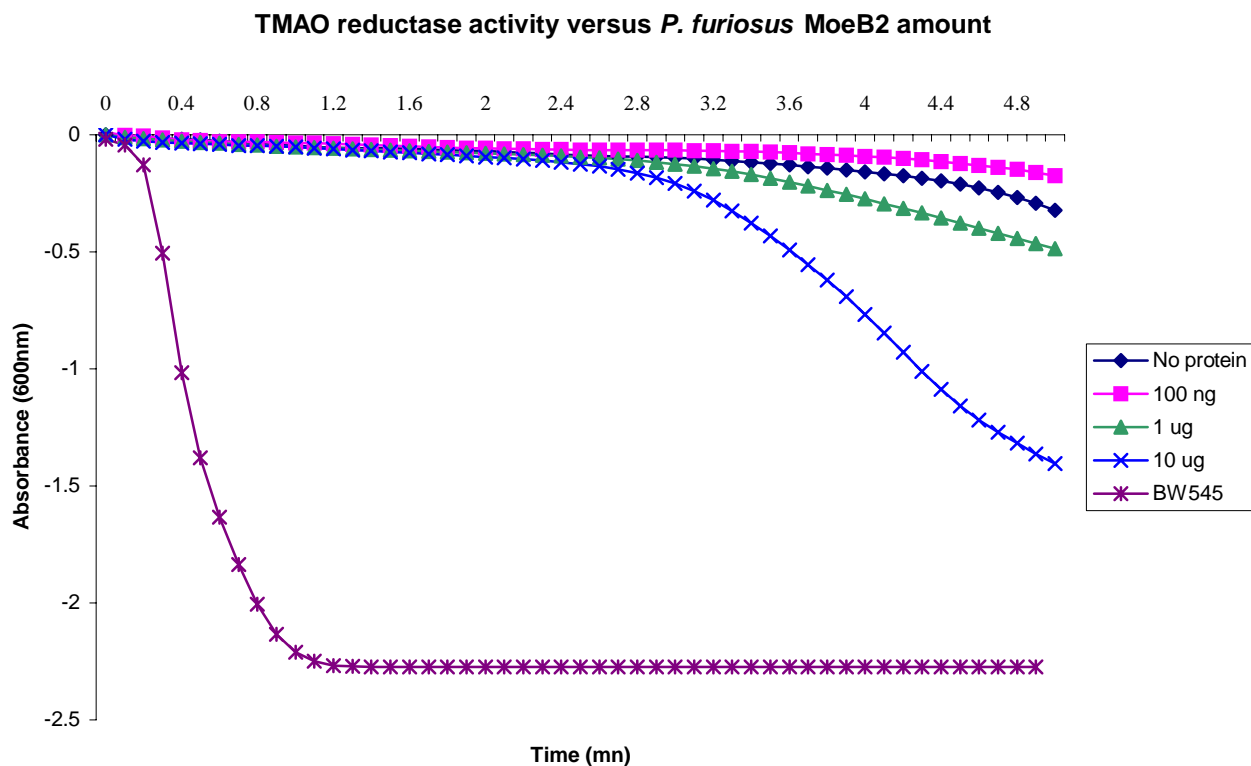


Figure 10: *In vitro* complementation of *E.coli moeB* mutation with *P. furiosus* MoeB2 detected using TMAO reductase assays. *E.coli moeB* mutant cells were grown in the presence of molybdenum. Specific activities were determined by the measuring the oxidation of reduced benzyl viologen at 600 nm coupled to the reduction of TMAO.

TMAO reductas activity versus *P. furiosus* MoeB2 amount

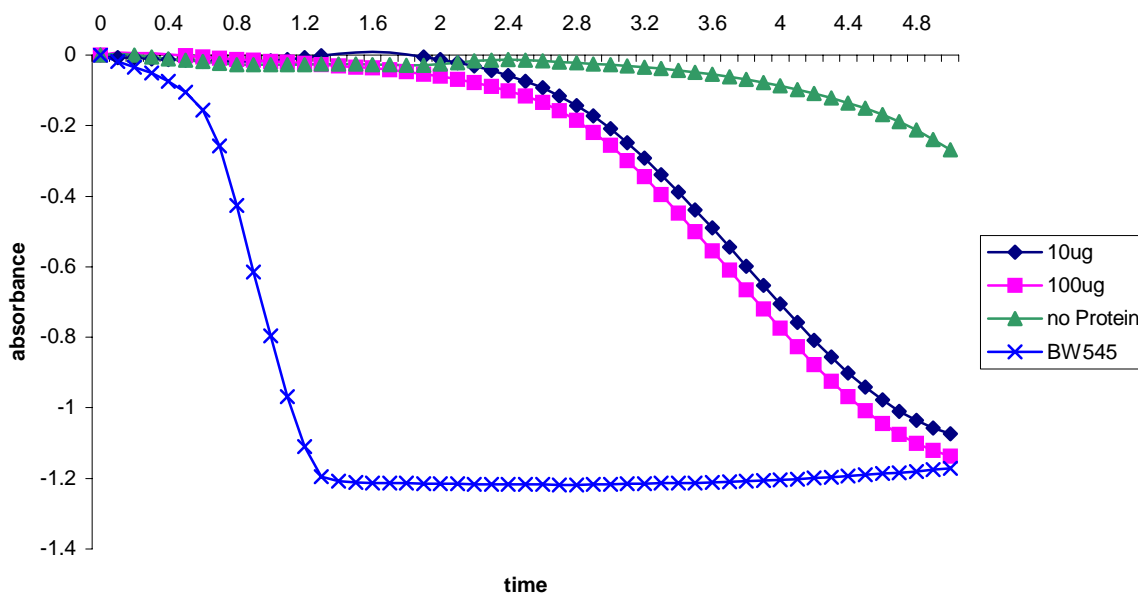


Figure 11: In Vitro complementation of *E.coli moeB* mutation with *P. furiosus* MoeB2 detected with TMAO reductase assays. *E.coli moeB* mutant cells were grown in the presence of tungsten. Specific activities were determined by the measuring the oxidation of reduced benzyl viologen at 600 nm coupled to the reduction of TMAO.

Table 3. In Vivo complementation of *E.coli moeA* mutations with *P. furiosus* MoeA, MoeA2 determined by restoration of nitrate reductase activities. The specific activities were obtained by using a nitrite colorimetric method.

Strain	Genotype	NR specific activity ^a
BW545	MoeA ⁺	152
AH215	MoeA ⁻	3.5
AH215/pELM3	MoeA ⁻ / +Pf MoeA2	50.2
AH215/pELM1	MoeA ⁻ / +Pf MoeA	3.1

^a nmol nitrite / min*mg. The reported specific activities represent an average of three separate experiments with the individual values varying by less than 10%.

Table 4: *In vitro* TMAO activity versus *P. furiosus* MoeA2 amount when assayed in the presence of molybdenum.

Sample	Specific Activity (nmol TMAO reduced/min*mg)
BW 545	2374.85
No protein	0
100 ng MoeA2	0.06
500 ng MoeA2	2.19
1 μ g MoeA2	7.65
10 μ g MoeA2	40.97
50 μ g MoeA2	17.99

Table 5: *In vitro* TMAO activity versus *P. furiosus* MoeA2 amount when assayed in the presence of tungsten.

Sample	Specific Activity (nmol TMAO reduced/min*mg)
BW545	1297
No protein	0
1 μ g MoeA2	No activity
10 μ g MoeA2	2.07
50 μ g MoeA2	No Activity

Table 6: *In vitro* TMAO activity versus *P. furiosus* MoeB2 amount when assayed in the presence of molybdenum.

Sample	Specific Activity (nmol/min*mg)
BW 545	2731.08
No protein	0
100 ng MoeB2	No Activity
1 µg MoeB2	1.07
10 µg MoeB2	6.33

Table 7: *In vitro* TMAO activity versus *P. furiosus* MoeB2 amount when assayed in the presence of tungsten.

Sample	Specific Activity (nmol/min*mg)
BW 545	1297.29
No protein	0
10 μ g MoeB2	5.70
100 μ g MoeB2	6.01

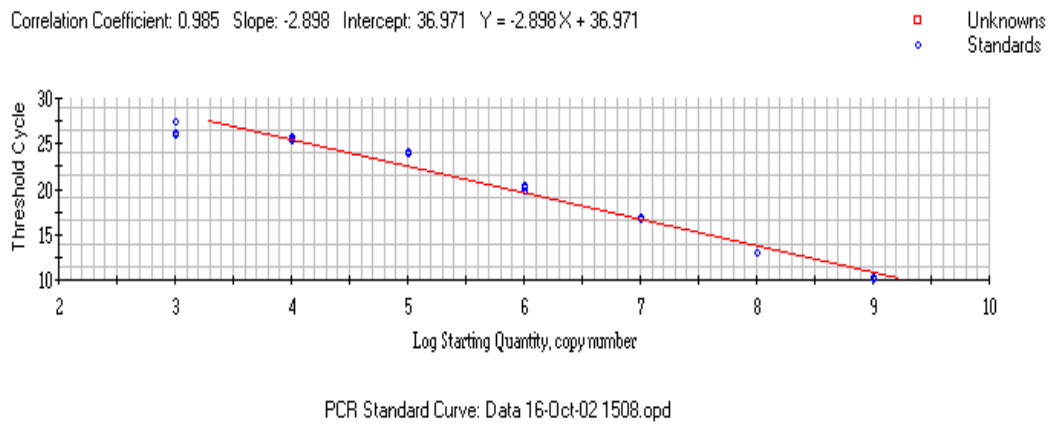
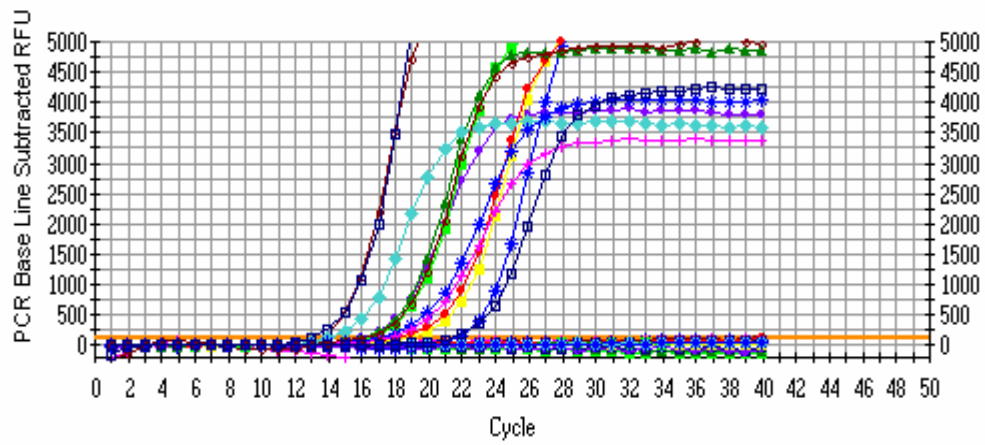


Figure 12. Standard curve for the real time RT-PCR experiments



PCR Amplification vs Cycle: Data 29-Oct-08 1216.opd

Figure 13. Real time RT-PCR threshold cycle data for cells grown in 1 nM tungsten.

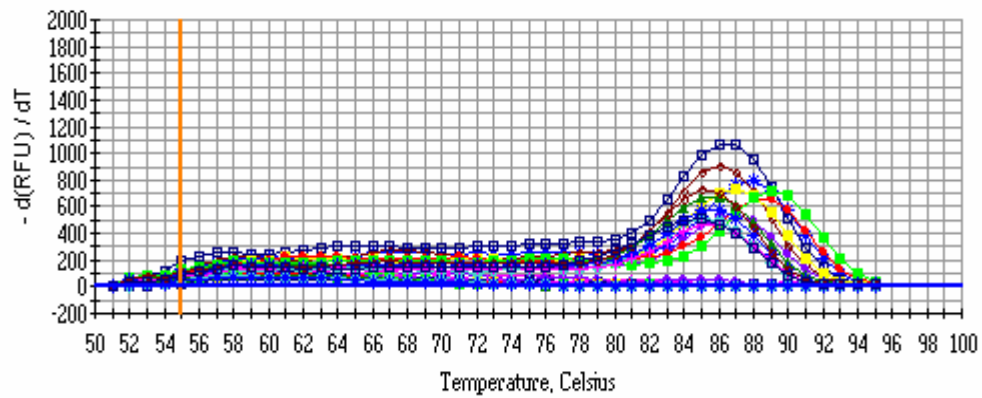


Figure 14. Real time RT-PCR melting curve for cells grown in 1 nM tungsten.

Tungsten cofactor synthesis genes	100 pM W average threshold cycle	1 nM W average threshold cycle	100 nM W average threshold cycle	10 μM W average threshold cycle	1 mM W average threshold cycle
MoeA	14.6	14.8	14.9	15.1	15.2
MoeA2	12.9	12.9	12.9	12.3	12.3
ModB	13.3	14.8	13.7	13.1	13.7
MoeB2	14.1	14.4	13.9	14.3	14.4
MoaB	12.3	12.4	13.0	12.5	11.8
MoaD2	16.8	16.7	15.8	14.9	18.4
MoaC	14.9	15.2	15.0	15.8	14.3
GAPOR	10.3	10.3	10.1	10.4	10.6

Table 8. Average threshold cycle for individual tungsten cofactor synthesis genes with various amounts of tungsten.

Tungsten cofactor synthesis genes	100 pM W initial mRNA copy number	1 nM W initial mRNA copy number	100 nM W initial mRNA copy number	10 μM W initial mRNA copy number	1 mM W initial mRNA copy number
MoeA	$1 \times 10^{7.1}$	$1 \times 10^{7.4}$	$1 \times 10^{7.3}$	$1 \times 10^{7.3}$	$1 \times 10^{7.2}$
MoeA2	$1 \times 10^{8.0}$	$1 \times 10^{8.0}$	$1 \times 10^{8.0}$	$1 \times 10^{8.2}$	$1 \times 10^{8.2}$
ModB	$1 \times 10^{7.9}$	$1 \times 10^{7.4}$	$1 \times 10^{7.7}$	$1 \times 10^{7.9}$	$1 \times 10^{7.7}$
MoeB2	$1 \times 10^{7.6}$	$1 \times 10^{7.5}$	$1 \times 10^{7.7}$	$1 \times 10^{7.5}$	$1 \times 10^{7.5}$
MoaB	$1 \times 10^{8.2}$	$1 \times 10^{8.1}$	$1 \times 10^{8.0}$	$1 \times 10^{8.1}$	$1 \times 10^{8.3}$
MoaD2	$1 \times 10^{6.7}$	$1 \times 10^{6.7}$	$1 \times 10^{7.0}$	$1 \times 10^{7.3}$	$1 \times 10^{6.1}$
MoaC	$1 \times 10^{7.3}$	$1 \times 10^{7.2}$	$1 \times 10^{7.3}$	$1 \times 10^{7.0}$	$1 \times 10^{7.5}$
GAPOR	$1 \times 10^{8.9}$	$1 \times 10^{8.9}$	$1 \times 10^{8.9}$	$1 \times 10^{8.9}$	$1 \times 10^{8.8}$

Table 9: Average mRNA copy number for individual tungsten cofactor synthesis genes with various amounts of tungsten.

Tungsten cofactor synthesis gene expression levels in response to varying amounts of tungsten in the growth media

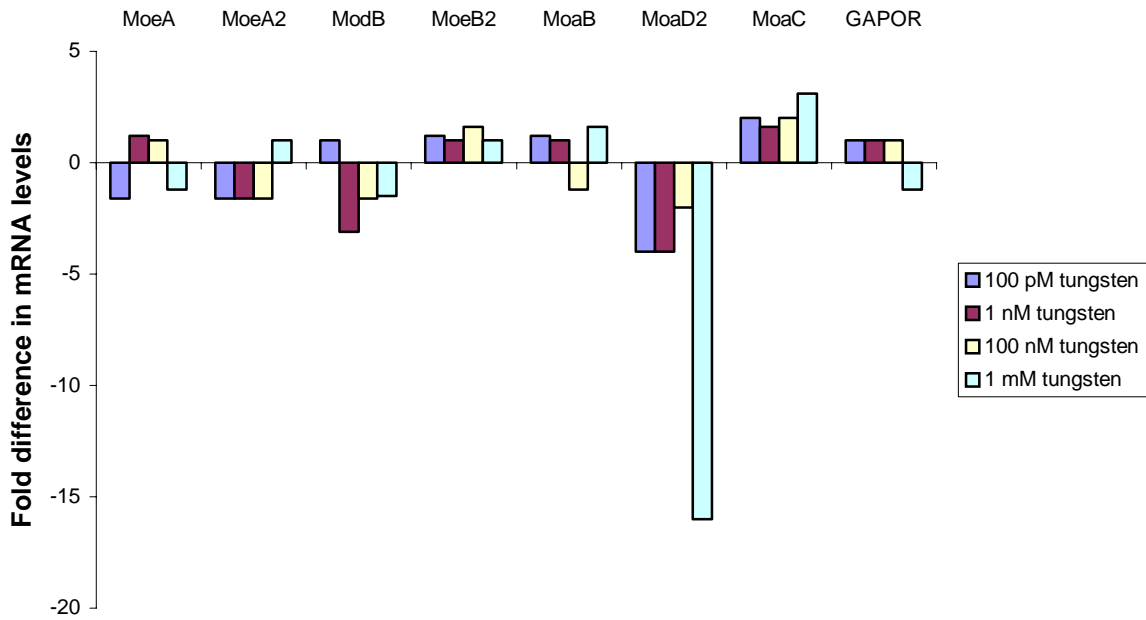


Figure 15. Tungsten cofactor synthesis gene expression levels in response to varying amounts of tungsten in the growth media. The mRNA obtained from each growth condition was compared to the mRNA isolated from cells grown in 10 μ M tungsten. A one-fold difference indicates that the same amount of mRNA was detected in both of the growth conditions.

Discussion

Biochemical and physiological studies of *P. furiosus* have determined that tungsten is required for growth (Munkund and Adams, 1996). This obligate tungsten requirement is most likely in part due to the replacement in *P. furiosus* of the classical glycolytic enzyme glyceraldehyde-3-phosphate dehydrogenase with the tungsten-containing enzyme glyceraldehyde-3-phosphate:ferredoxin oxidoreductase (Mukund and Adams, 1995). In order to begin to understand *P. furiosus* physiology it would be beneficial to decipher how the tungsten cofactor biosynthesis occurs. To begin this task, a number of MoCo biosynthesis homologs were identified in *P. furiosus*. It was quickly noticed that there were multiple MoeA and MoeB homologs. Unfortunately, due to the lack of a genetic system in *P. furiosus*, direct probing of function of the MoCo biosynthesis genes was not feasible. So in order to find which of the putative homologs are true homologs, complementation studies were used.

Partial complementation of defects in *E.coli moeA* was observed in nitrate reductase assays including *P. furiosus* MoeA2. The *in vivo* nitrate reductase assays indicated that *P. furiosus* MoeA2 could support one-third the activity that was seen in wild type *E. coli*. The *in vitro* nitrate reductase assays show that *P. furiosus* MoeA2 could support one-tenth the activity seen in wild type *E. coli*. When *in vitro* *P. furiosus* MoeA2 nitrate reductase activity is compared to the wild type nitrate reductase activity there is a dramatic decrease as opposed to the *in vivo* assays. But when comparing *P. furiosus* MoeA2 complemented nitrate reductase activity to *E. coli* MoeA complemented nitrate reductase activity there is only a 4.23 nmole NO₂⁻•min⁻¹•mg⁻¹ decrease. One factor in the decreased activity for both the *in vitro* *P. furiosus* MoeA2 and the *E.coli* MoeA as compared to the wild type activity may be explained by results found by Magalon et al. Their results suggest that, *in vivo*, molybdenum

cofactor biosynthesis occurs on protein complexes, such as MoeA-MoaD complexes, rather than by separate action of molybdenum cofactor biosynthesis proteins (Magalon et al 2002). Because the MoCo biosynthesis protein complexes appear to be critical to MoCo synthesis it is thought that greater complementation might be observed with *P. furiosus* MoCo homologs if multiple *P. furiosus* MoCo synthesis enzymes were included. As it is likely that various *P. furiosus* would be capable of interacting to a greater degree than would be expected for interactions between *P. furiosus* and *E. coli* MoCo synthesis proteins.

Defects in *E. coli moeA* were partially complemented in the TMAO reductase assays including *P. furiosus* MoeA2. For the TMAO reductase assays with molybdenum the wild type had a specific activity of 2,374 nmole TMAO reduced $\cdot\text{min}^{-1}\cdot\text{mg}^{-1}$ and assays with 10 μg MoeA2 had a specific activity of 40.97 nmole TMAO reduced $\cdot\text{min}^{-1}\cdot\text{mg}^{-1}$. However, with the TMAO assays with tungsten, the wild type had a specific activity of 1,297 nmole TMAO reduced $\cdot\text{min}^{-1}\cdot\text{mg}^{-1}$ and assays with 10 μg MoeA2 had an activity of 2.07 nmole TMAO reduced $\cdot\text{min}^{-1}\cdot\text{mg}^{-1}$. With molybdenum *P. furiosus* MoeA2 has about one sixtieth of activity of the wild type *E. coli* activity as opposed to with tungsten *P. furiosus* MoeA2 which has approximately one six-hundredth the activity of the wild type *E. coli*. Unfortunately, due to limited supply of purified *P. furiosus* MoeA, we were unable to rule out the possibility that *P. furiosus* MoeA could substitute functionally for *E. coli* MoeA when a tungsten cofactor is synthesized, as those experiments have not been completed. By analyzing the sequence alignments of the *P. furiosus* MoeA, *P. furiosus* MoeA2 and *E. coli* MoeA (Figures 16 and 17) we are unable to distinguish which of the *P. furiosus* MoeA putative homologs would act as the true homolog based strictly on conservation of key catalytic/functional amino acid residues. Both *P. furiosus* MoeA and *P. furiosus* MoeA2 contain the conserved residues that

have been defined as critical for *E. coli* MoeA function (Asp-59, Thr-100, Asp-142, Glu-188, Asn-205, Asp 228 and Ser-371). Although a molybdoenzyme has yet to be characterized in *P. furiosus* one cannot rule out the fact that it could exist, there are still at least two putative tungstoenzymes that have not been characterized (currently annotated as WOR4 and WOR5 in the *P. furiosus* database) and their metal centers have yet to be explored. This could be a reasonable explanation for the presence of the two MoeA homologs in *P. furiosus* if one is specific for activation of tungsten and the other for activation of molybdenum.

Partial complementation of defects in *E.coli moeB* was observed in *in vitro* nitrate reductase assays including 100 μg *P. furiosus* MoeB2 and 50 μg *E.coli* MoeB which supported 19.6, and 24 $\text{nmole NO}_2^- \cdot \text{min}^{-1} \cdot \text{mg}^{-1}$ of activity respectively. However, both *P. furiosus* MoeB and *E. coli* ThiF supported less than one $\text{nmole NO}_2^- \cdot \text{min}^{-1} \cdot \text{mg}^{-1}$ of activity. The data from the *P. furiosus* MoeB2 *in vitro* nitrate reductase assays are similar to the *in vitro* *P. furiosus* MoeA2 assays. When the nitrate reductase activities supported by *P. furiosus* MoeB2 is compared to that of wild type *E.coli* the *P. furiosus* MoeB2 supports only one sixth of the activity. But when *P. furiosus* MoeB2 activity is compared to the *E.coli* MoeB activity there is only a 4.4 $\text{nmole NO}_2^- \cdot \text{min}^{-1} \cdot \text{mg}^{-1}$ difference. This suggests that *P. furiosus* MoeB2 is the true *E.coli* MoeB homolog.

Defects in *E.coli moeB* were partially complemented in the TMAO reductase assays including *P. furiosus* MoeB2. For the TMAO reductase assays with molybdenum the wild type had a specific activity of 2,374 $\text{nmole TMAO reduced} \cdot \text{min}^{-1} \cdot \text{mg}^{-1}$ and assays with 10 μg MoeB2 had a specific activity of 6.33 $\text{nmole TMAO reduced} \cdot \text{min}^{-1} \cdot \text{mg}^{-1}$. However, with the TMAO assays with tungsten, the wild type had a specific activity of 1,297 nmole TMAO

reduced $\cdot\text{min}^{-1}\cdot\text{mg}^{-1}$ and assays with 100 μg MoeB2 had an activity of 6.0 nmole TMAO reduced $\cdot\text{min}^{-1}\cdot\text{mg}^{-1}$.

P. furiosus MoeB has a lower similarity to *E. coli* MoeB (44%) than *P. furiosus* MoeB2 (50%) and because *P. furiosus moeB* is located next to ThiI in the *P. furiosus* genome it is believed that the *P. furiosus* MoeB serves as the *E. coli* ThiF homolog even though it is annotated as MoeB in the *P. furiosus* genomic database. When comparing the sequence alignments of *P. furiosus* MoeB and *E. coli* ThiF (Figure 18) the cysteine residue that is required as for thiazole biosynthesis is present in both *P. furiosus* MoeB and *E. coli* ThiF, but this cysteine residue is not present in the *P. furiosus* MoeB2 sequence (Figure 20). Figure 18 shows that *P. furiosus* MoeB contains the conserved metal-binding CXXC motifs that are seen with in *E. coli* ThiF while *P. furiosus* MoeB2 does not have these motifs. Figure 19 further indicates that *P. furiosus* MoeB may not be the true homolog for *E. coli* MoeB, since an amino acid residue (cysX) that is required for the adenylation of MoaD by *E. coli* MoeB but is not conserved in *P. furiosus* MoeB. However, *P. furiosus* MoeB2 does contain all of the residues defined as critical for the adenylation of MoaD by *E. coli* MoeB (Figure 21).

The tungsten cofactor genes do not seem to be regulated like the molybdenum cofactor genes in *E. coli*. Within the molybdenum system when there is an increase in the amount of molybdenum added to the growth media there is an increase in the molybdenum cofactor synthesis genes and a decrease in the molybdenum transporter gene production. These changes help the cell from becoming overwhelmed with molybdenum, which in high concentration can be toxic to the cell. However, the tungsten cofactor genes do not seem to have this type of regulation. Figure 15 shows that there is little difference between the mRNA grown in the various amounts of tungsten. If the tungsten cofactor genes were

regulated like the molybdenum genes there would be a decrease in ModB, part of the tungsten transporter, as the amount of tungsten went up. However, one must keep in mind that ModB is only a putative homolog and it has not been proven that it is part of the tungsten transporter, there is a possibility that it is a part of another transport system. If ModB is part of another transporter system it would make sense that it was not affected by the varying amount of tungsten added to the growth media. The only gene that seems to have a significant difference is MoadD2, it had a 16-fold decrease when 1 mM tungsten was added to the growth media (Figure 15). The reasoning behind this decrease is still to be determined and will have to be looked at in future studies.

Although the complementation of the *E. coli moeA* and *moeB* defects by the *P. furiosus* homologs MoeA2 and MoeB2 did not fully restore wild type nitrate reductase activity and TMAO reductase levels, the partial restoration does demonstrate that these *P. furiosus* homologs can function in these putative roles and therefore likely serve these same functions in *P. furiosus*. The lower amount of activity observed for the *P. furiosus* proteins compared to their wild type *E. coli* counterparts could be attributed to several different reasons. First, the complementation experiments were performed at 37°C, which is far below the optimal temperature normally seen for *P. furiosus* proteins (~ 90 °C to 100 °C). Secondly, the lower activity may be due in part to the use of molybdenum in the assays rather than tungsten. Since, *P. furiosus* has been shown to only contain tungstoenzymes, it is reasonable to presume that the *P. furiosus* cofactor synthesis genes are optimized for functioning with tungsten rather than molybdenum. However, only molybdenum can support *E. coli* nitrate reductase activity, and therefore, molybdenum was used in the assays in place of tungsten.

Future work in this area will include further functional characterization of the *P. furiosus* MoeA and MoeB proteins using tungsten-based TMAO reductase activity assays as well as the characterization of the other putative *P. furiosus* tungsten cofactor proteins. Once the genes that are involved in the tungsten cofactor synthesis are defined, further experiments will be performed to determine the expression patterns of these genes to establish whether these tungsten cofactor synthesis genes are regulated in a manner similar to that seen for the molybdenum cofactor genes in mesophilic bacteria.

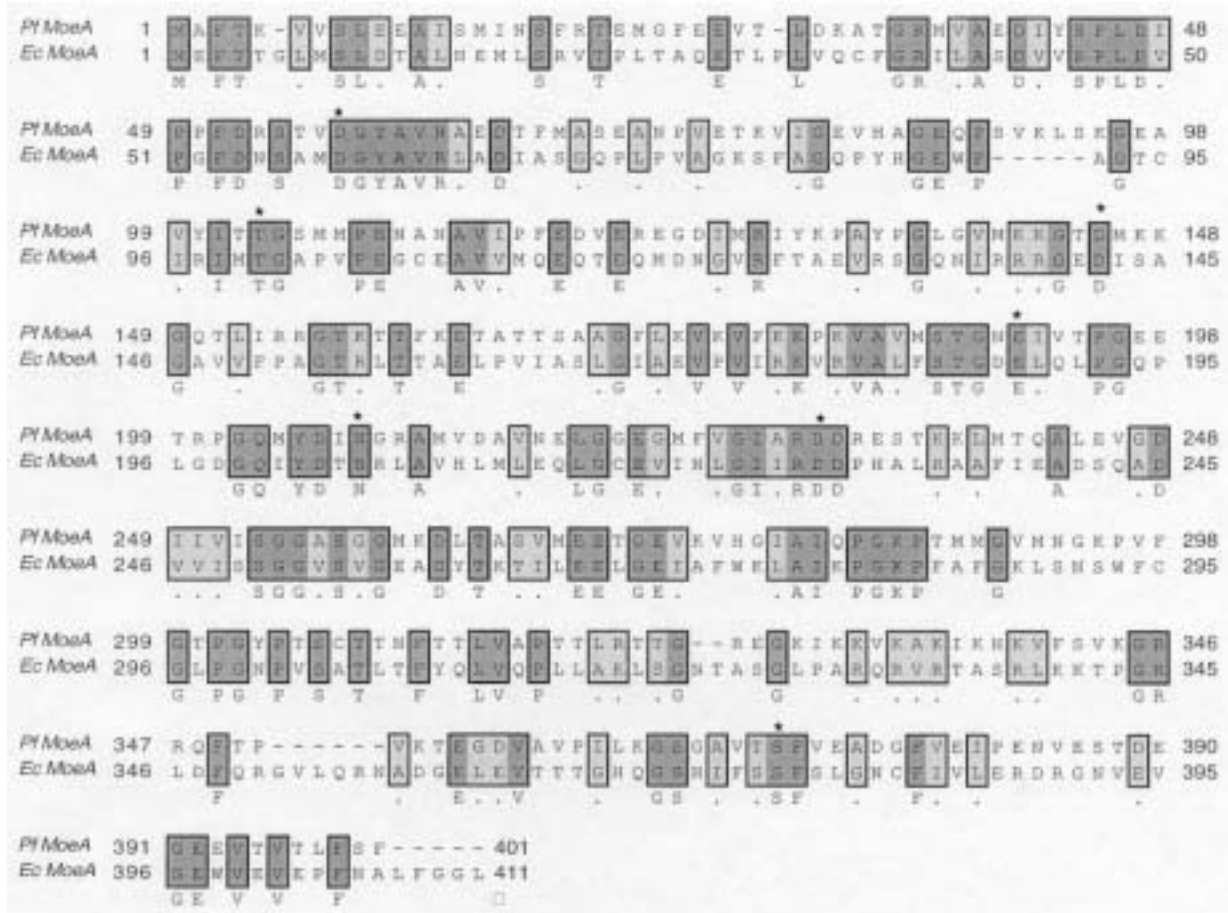


Fig. 16. Alignment of *P. furiosus* MoeA with *E. coli* MoeA. Identical residues are indicated by dark shading and similar residues with light shading. Asterisks denote conserved residues that have been defined as critical for *E. coli* MoeA function.

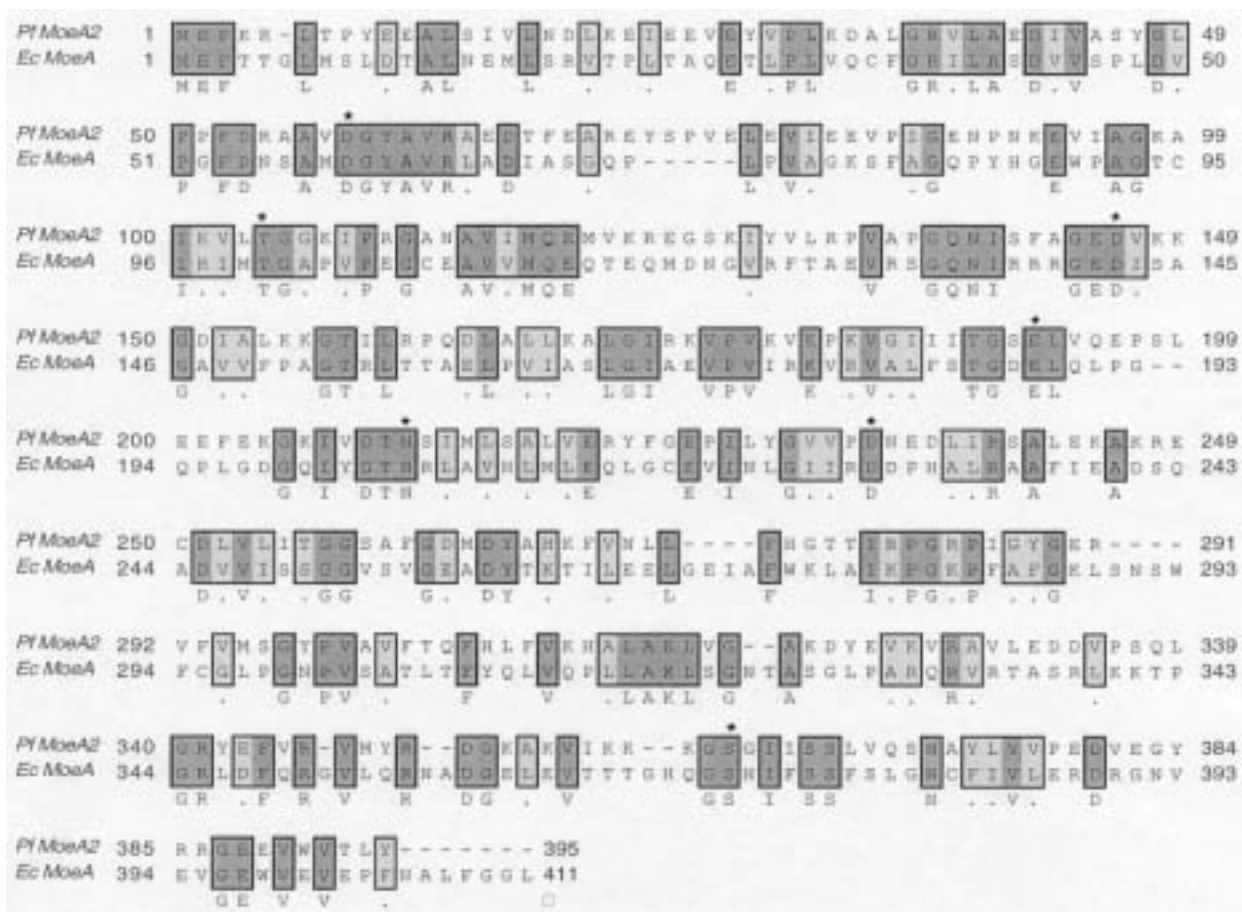


Fig. 17. Alignment of *P. furiosus* MoeA2 with *E. coli* MoeA. Identical residues are indicated by dark shading and similar residues with light shading. Asterisks denote conserved residues that have been defined as critical for *E. coli* MoeA function.

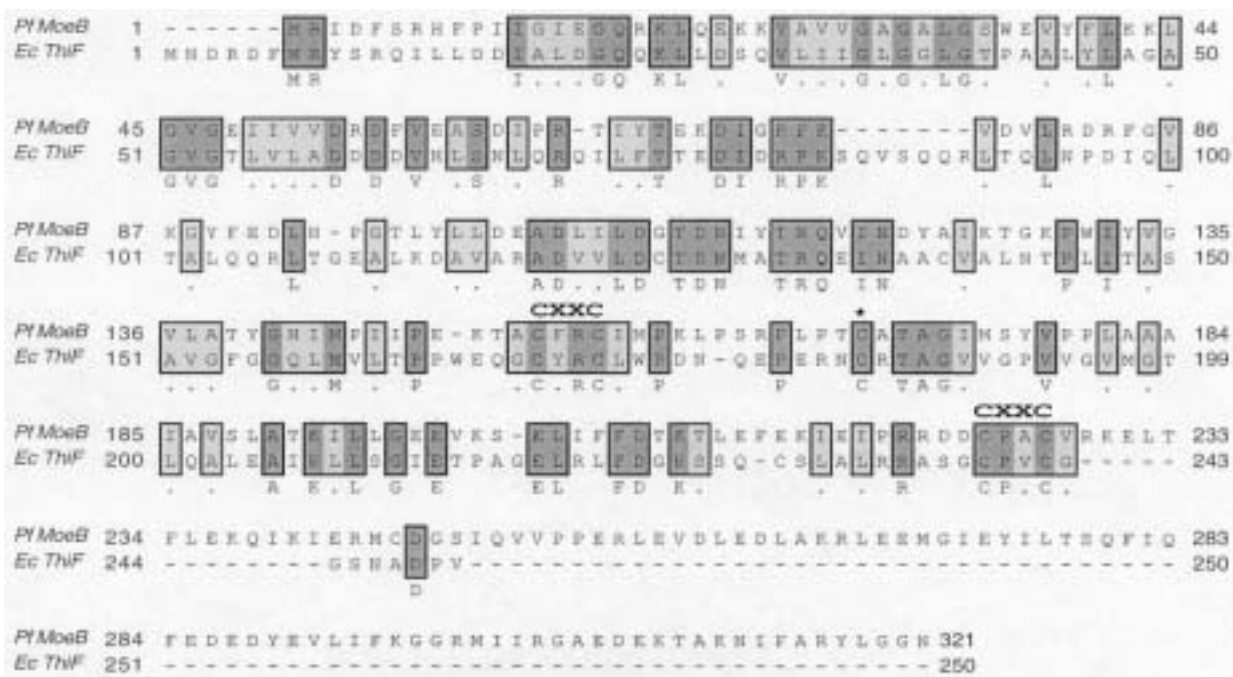


Fig. 18. Alignment of *P. furiosus* MoeB with *E. coli* ThiF. Identical residues are indicated by dark shading and similar residues with light shading. The Asterisk denotes the conserved cysteine residue that is required as for thiazole biosynthesis by *E. coli* ThiF. Conserved metal-binding CXXC motifs are also marked.

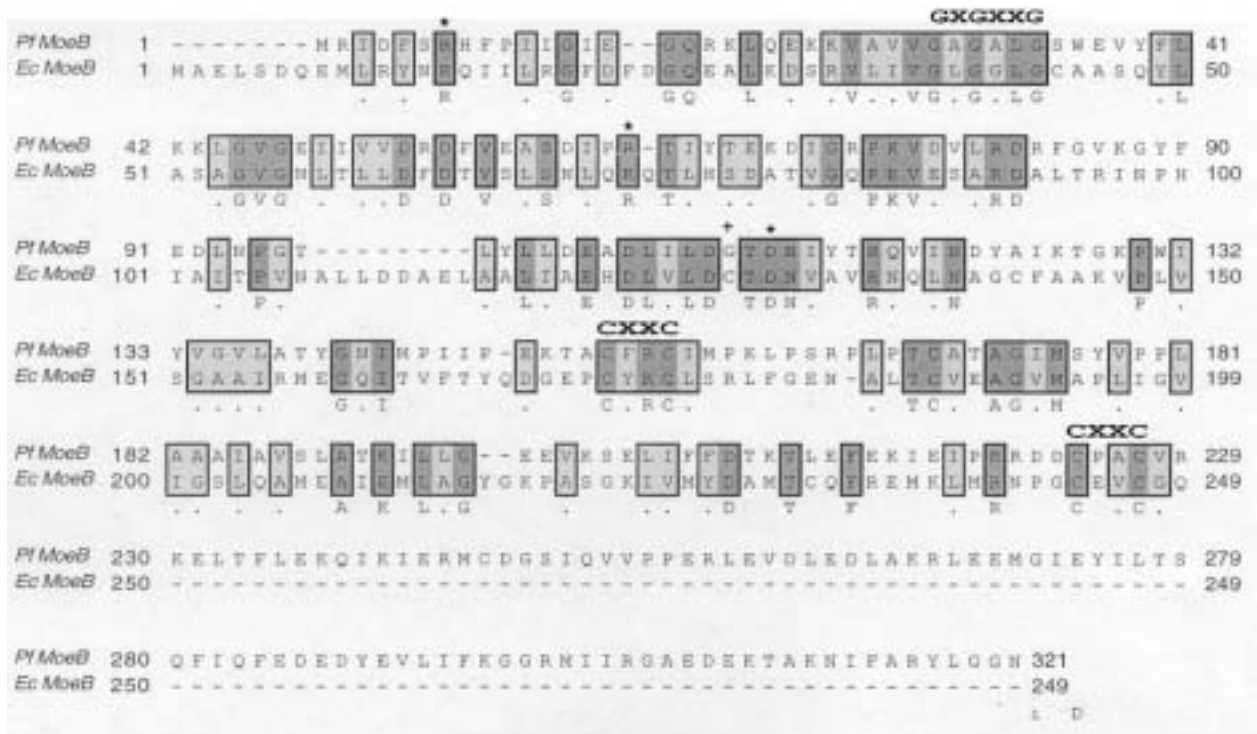


Fig. 19. Alignment of *P. furiosus* MoeB with *E. coli* MoeB. Identical residues are indicated by dark shading and similar residues with light shading. Asterisks denote conserved residues that have been defined as critical for the adenylation of MoaD by *E. coli* MoeB. The plus sign (+) indicates an amino acid residue that is required for the adenylation of MoaD by *E. coli* MoeB which is not conserved in *P. furiosus* MoeB. The conserved ATP-binding motif, GXXGXXG, is shown as are two conserved Zn-binding CXXC domains.

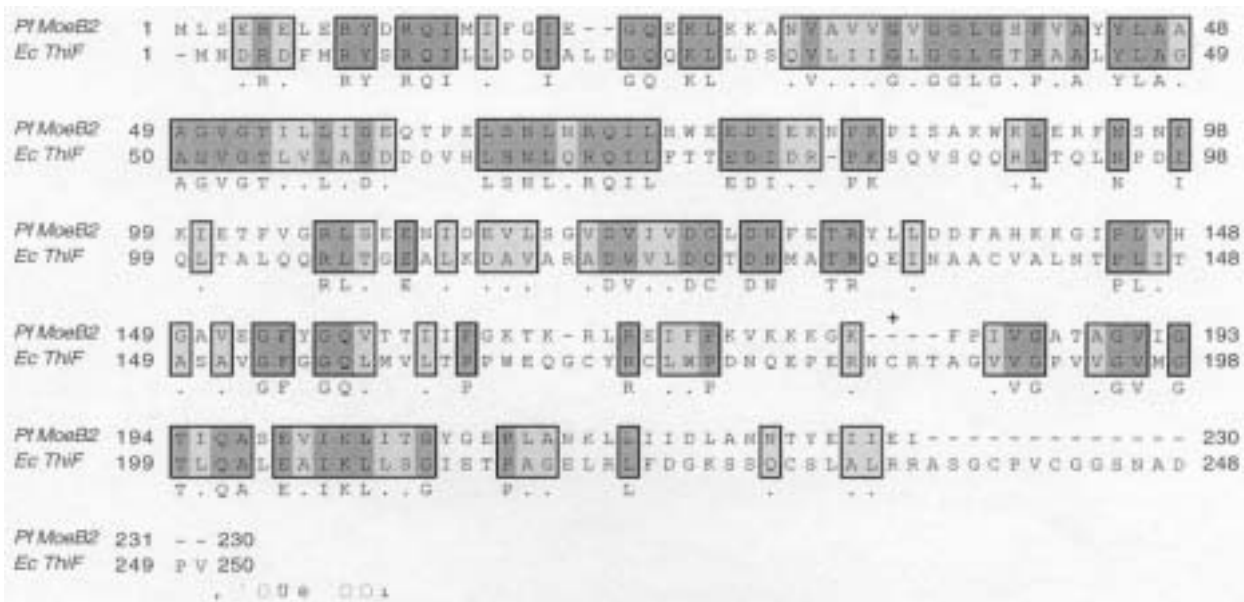


Fig. 20. Alignment of *P. furiosus* MoeB2 with *E. coli* ThiF. Identical residues are indicated by dark shading and similar residues with light shading. The plus sign (+) marks the location of the cysteine residue that is required as for thiazole biosynthesis.

Literature cited

- Adams MWW (1999) The biochemical diversity of life near and above 100 degrees C in marine environments. *Journal of Applied Microbiology* 85:108S-117S
- Anderson L, McNairn E, Leubke T, Pau R, and Boxer D (2000) ModE -dependant molybdate regulation of the molybdenum cofactor operon *moa* in *Escherichia coli* *Journal of bacteriology* 182: 7035-7043
- Appleyard M, Sloan J, Hana'n G, Heck I, Kinghorn J, and Unkles S (1998) The *Aspergillus nidulans cnxF* gene and its involvement in molybdopterin biosynthesis *JBC* 273:14869-14876
- Arnulf K, Adams MW (1996) Tungsten in biological systems. *FEMS Microbiology Reviews*.18:5-63.
- Buc J, Santini CL, Giordani R, Czjzek M, Wu LF, Giordano G (1999) Enzymatic and physiological properties of the tungsten-substituted molybdenum TMAO reductase from *Escherichia coli*. *Mol Microbiol* 32:159-168.
- Chan MK, Mukund S, Kletzin A, Adams MW, Rees DC (1995) Structure of a hyperthermophilic tungstopterin enzyme, aldehyde ferredoxin oxidoreductase. *Science* 267:1463-1469.
- Fiala G, Stetter KO (1986) *Pyrococcus-Furiosus* Sp-Nov Represents a Novel Genus of Marine Heterotrophic Archaeobacteria Growing Optimally at 100-Degrees C. *Archives of Microbiology* 145:56-61

- Gallois P, Makishima T, Hecht V, Despres B, Laudie M, Nishimoto T, Cooke R (1997) An *Arabidopsis thaliana* cDNA complementing a hamster apoptosis suppressor mutant. *Plant J* 6:1325-31.
- Grunden A, Ray R, Rosentel J, Healy F, Shanmugam K. Repression of the *Escherichia coli* *modABCD* (molybdate transport) operon by ModE. *J Bacteriol.* 1996 Feb;178(3):735-44.
- Grunden A, Self W, Villain M, Blalock J, and Shanmugam (1999) An analysis of the binding of repressor protein ModE to *modABCD* (molybdate transport) operator /promoter DNA of *Escherichia coli* *Journal of biological chemistry* 34:24308-24315
- Hasona A, Ray RM, Shanmugam KT (1998) Physiological and genetic analyses leading to identification of a biochemical role for the *moeA* (molybdate metabolism) gene product in *Escherichia coli*. *J Bacteriol* 180:1466-1472.
- Hasona A, Self W, and Shanmugam (2001) Transcriptional regulation of the *moe* (molybdate metabolism) operon of *Escherichia coli*. *Arch Microbiol.* 175: 178-88.
- Johnson JL, Indermaur LW, Rajagopalan KV (1991) Molybdenum cofactor biosynthesis in *Escherichia coli*. Requirement of the *chlB* gene product for the formation of molybdopterin guanine dinucleotide. *J Biol Chem* 266:12140-12145.
- Joshi MS, Johnson JL, Rajagopalan KV (1996) Molybdenum cofactor biosynthesis in *Escherichia coli* *mod* and *mog* mutants. *J Bacteriol* 178:4310-4312.
- Kletzin A, Adams MWW (1996) Tungsten in biological systems. *Fems Microbiology Reviews* 18:5-63
- Leimkuhler S, Angermuller S, Schwarz G, Mendel R, and Klipp W (1999) Activity of the molybdopterin containing xanthine dehydrogenase of *Rhodobacter capsulatus* can be

- restored by high molybdenum concentrations in *moeA* Mutant defective in molybdenum cofactor biosynthesis *J Bacteriol* 181:5930-5939
- Leimkühler S, Wuebbens M, Rajagopalan (2001) Characterization of *Escherichia coli* MoeB and its involvement in the activation of molybdopterin synthase for the biosynthesis of the molybdenum cofactor *JBC* 37: 34695-34701
- Magalon A, Frixon C, Pommier J, Giordano G and Blasco F (2002) In vivo interactions between gene products involved in the final stages of molybdenum cofactor biosynthesis in *Escherichia coli* *J Biol Chem.* [epub ahead of print]
- McNicholas P, Rech S, Gunsalus R. Characterization of the ModE DNA-binding sites in the control regions of *modABCD* and *moaABCDE* of *Escherichia coli*. *Mol Microbiol.* 1997 Feb;23(3):515-24.
- Mukund S, Adams MW (1991) The novel tungsten-iron-sulfur protein of the hyperthermophilic archaeobacterium, *Pyrococcus furiosus*, is an aldehyde ferredoxin oxidoreductase. Evidence for its participation in a unique glycolytic pathway. *J Biol Chem* 266:14208-14216.
- Mukund S, Adams MW (1995) Glyceraldehyde-3-phosphate ferredoxin oxidoreductase, a novel tungsten-containing enzyme with a potential glycolytic role in the hyperthermophilic archaeon *Pyrococcus furiosus*. *J Biol Chem* 270:8389-8392.
- Mukund S, Adams MW (1996) Molybdenum and vanadium do not replace tungsten in the catalytically active forms of the three tungstoenzymes in the hyperthermophilic archaeon *Pyrococcus furiosus*. *J Bacteriol* 178:163-167.

- Nicholas DJD, Nason A (1957) Determination of Nitrate and Nitrite. *Methods in Enzymology* 3:981-984
- Nohno T, Kasai Y, Saito T (1998) Cloning and sequencing of the *Escherichia coli chlEN* operon involved in molybdopterin biosynthesis. *J Bacteriol* 170:4097-4102
- Palmer T, Santini CL, Iobbi-Nivol C, Eaves DJ, Boxer DH, Giordano G (1996) Involvement of the narJ and mob gene products in distinct steps in the biosynthesis of the molybdoenzyme nitrate reductase in *Escherichia coli*. *Mol Microbiol* 20:875-884.
- Pitterle J, and Rajagopalan K, (1989) Two proteins encoded at the *chlA* locus constitute the converting factor of *Escherichia coli chlAII* *J Bacteriol* 171:3373-3378
- Pitterle DM, Johnson JL, Rajagopalan KV (1993) In vitro synthesis of molybdopterin from precursor Z using purified converting factor. Role of protein-bound sulfur in formation of the dithiolene. *J Biol Chem* 268:13506-13509.
- Pitterle DM, Rajagopalan KV (1993) The biosynthesis of molybdopterin in *Escherichia coli*. Purification and characterization of the converting factor. *J Biol Chem* 268:13506-13509.
- Prior P, Schmitt B, Grenningloh G, Pribilla I, Malthaup G, Beyeuther K, Maulet Y, Werner P, Langosch D Kirsch J (1992) Primary structure and alternative splicing variants of gephyrin, a putative glycine receptor-tubulin linker protein. *Neuron* 8:1161-1170
- Rajagopalan KV (1997) Biosynthesis and processing of the molybdenum cofactors. *Biochem Soc Trans* 25:757-761.
- Rajagopalan KV, Johnson JL (1992) The pterin molybdenum cofactors. *J Biol Chem* 267:10199-10202.

- Rieder C et al. (1998) Rearrangement reactions in the biosynthesis of molybdopterin--an NMR study with multiply $^{13}\text{C}/^{15}\text{N}$ labelled precursors. *Eur J Biochem* 255:24-36.
- Roy R, Mukund S, Schut GJ, Dunn DM, Weiss R, Adams MW (1999) Purification and molecular characterization of the tungsten-containing formaldehyde ferredoxin oxidoreductase from the hyperthermophilic archaeon *Pyrococcus furiosus*: the third of a putative five-member tungstoenzyme family. *J Bacteriol* 181:1171-1180.
- Schrag J, Hauang W, Sivaraman J, Smith C, Plamandon J, Larocque R, Matte A, and Cygler M (2001) The crystal structure of *Escherichia coli* MoeA, a protein from the molybdopterin synthesis pathway. *J. Mol. Biol* 310:419-431
- Self WT, Grunden A, Hasona A, Shanmugam K (1999) Transcriptional regulation of molybdoenzyme synthesis in *Escherichia coli* in response to molybdenum: MoeA molybdate a repressor of the mod ABCD (molybdate transport) operon us a secondary transcriptional activator for the *hyc* and *nar* operons. *Microbiology* 145:41-55
- Stallmeyer B, Nerlich A, Schiemann J, Brinkmann H, and Mendel R (1995) Molybdenum cofactor biosynthesis: the *Arabidopsis thaliana* cDNA *cnx1* encodes a multifunctional two domain protein homologous to a mammalian neuroprotein, the insect protein cinnamon and three *Escherichia coli* proteins. *Plant J* 8:101-112
- Stallmeyer B, Schwarz G, Schulze J, Nerlich A, Reiss J, Kirsch J, and Mendel R (1999) THE neurotransmitter receptor-anchoring protein gephyrin reconstitutes molybdenum cofactor biosynthesis in bacteria, plants and animals. *Proc. Natl. Acad. Sci. USA* 96:1333-1338

- Stetter, K.O. (1996) Hyperthermophilic procaryotes. FEMS Microbiol. Rev, 18:149-158.
- Taylor S, Kelleher N, Kinsland C, Chiu H, Costello C, Backstrom A, McLafferty W, Begley T (1998) Thiamin biosynthesis in Escherichia coli identification of ThiS thiocarboxylate as the intermediate sulfur donor in the thiazole formation. Journal of Biological Chemistry. 273:16555-16560
- Vander Horn P, Backstrom A, Stewart V, and Begley T (1993) Structural studies for thiamine biosynthetic enzymes (*thi*CEFGH) J Bacteriol 175 982-992
- Varshavsky A (1997) The ubiquitin system. Trends Biochem Sci. 22:383-7.
- Woese CR, Kandler O and Wheelis ML. (1990) Towards a natural system of organisms: proposal for the domains Archaea, Bacteria, and Eucarya. Proc Natl Acad Sci U S A. 87(12): 4576-9.
- Wuebbens MM, Rajagopalan KV (1995) Investigation of the early steps of molybdopterin biosynthesis in Escherichia coli through the use of in vivo labeling studies. J Biol Chem 270:1082-1087.
- Xi J, GE Y, Kinsland C, McLafferty F, Begley T. (2001) Biosynthesis of the thiazole moiety of thianin in Escherichia coli: identification of an acyldisulfide-linked protein-protein conjugate that is functionally analogous to the ubiquitin/E1 complex. PNAS. 98:8513-8518.
- Xiang S, Ncchils J, Rajagopalan K, and Schindelin H (2001) The crystal structure of Escherichia coli MoeA and its relationship to the multifunctional protein gephyrin Structure 9:299-310